BNL 50421

OPERATING MANUAL FOR THE PSE&G HYDROGEN RESERVOIR CONTAINING IRON TITANIUM HYDRIDE

G. STRICKLAND AND J.J. REILLY

February 1974

BROOKHAVEN NATIONAL LABORATORY
ASSOCIATED UNIVERSITIES, INC.
UNDER CONTRACT NO. AT(30-1)-16 WITH THE
UNITED STATES ATOMIC ENERGY COMMISSION

BNL 50421
(Engineering and Equipment - TID-4500)

OPERATING MANUAL FOR THE PSE&G HYDROGEN RESERVOIR CONTAINING IRON TITANIUM HYDRIDE

G. STRICKLAND AND J.J. REILLY

February 1974

The work described was supported in part by the Public Service Electric & Gas Company of New Jersey, and in part by the U.S. Atomic Energy Commission.

BROOKHAVEN NATIONAL LABORATORY
UPTON, NEW YORK 11973

Printed in the United States of America
Available from
National Technical Information Service
U.S. Department of Commerce
5285 Port Royal Road
Springfield, Virginia 22151
Price: Printed Copy $4.00; Microfiche $1.45

May 1974 450 copies

CONTENTS

INTRODUCTION

This manual is written for personnel concerned with operation of the hydrogen reservoir which Brookhaven National Laboratory (BNL) built for Public Service Electric & Gas Co. (PSE & G) for use in their experimental energy-storage system. Information is provided on how the reservoir functions and how it can be safely operated. The equipment is described and basic operating procedures are given along with precautionary measures. Some of the material presented here will also appear in the project report, and some of the material will supplement that in the report. As operating experience is gained, more detailed procedures can be prepared for interfacing the reservoir with the other major components comprising the energy-storage system.

In combination with a water electrolyzer and a fuel-cell stack, the hydrogen reservoir provides a new way of storing energy. The reservoir is the storage unit in the system; it is used to store hydrogen from the electrolyzer and subsequently release it to the fuel-cell stack. In simple terms, a reservoir for hydrogen consists of a closed vessel filled with granular metal hydride and provided with a particle barrier, a gas connection, and a means of handling the necessary thermal load. In this case the hydrogen is stored as iron titanium hydride in a pressure vessel; porous metal tubing is used for the barrier, and an internal heat exchanger is provided to handle the thermal load. The hydride may be cycled many times provided gaseous impurities which degrade its performance are excluded from the system. Water at readily available temperatures (approximately 60° and 120°F) is suitable for use as the heat exchange medium.

The design of this reservoir was based on the capabilities of the electrolyzer and fuel-cell stack, but tests have shown that it can exceed their design specifications. It will take up H_2 at a rate >1.5 lb/hr, deliver it at a rate >1.0 lb/hr, and its working capacity is significantly more than the 10 lb of H_2 originally specified. A compressor (500-PSIG rating) is required to pressurize H_2 leaving the electrolyzer in order to obtain a practical sorption rate. The temperature and flow rate of the water in the heat exchanger tubes also are an important factor with respect to sorption and desorption rates.

HYDRIDE BEHAVIOR

For a detailed discussion of this subject the reader is referred to the Appendix. The basic reactions occurring in the reservoir may be summarized as follows:

$$1.08\ FeTiH_{0.1} + H_2 \rightleftharpoons 1.08\ FeTiH_{1.95}. \qquad \Delta H \cong 7.5\ Kcal$$

Heat must be removed in the forward reaction (hydriding or charging) and it must be supplied during the reverse reaction (dehydriding or discharging). The hydride decomposes readily and has a pressure dependent upon composition and temperature. This behavior is illustrated in Fig. 1 for charging and discharging H_2 under equilibrium conditions. The value of H/M, the hydrogen to metal (Fe + Ti) ratio, is half that of H in the formula $FeTiH_x$. The lower curve shows the dissociation pressure for the reverse reaction; and as shown, higher pressures exist during the forward reaction. The steep initial rise in pressure is the region of solid solution of H_2 in the metal lattice; the plateau is the region of FeTi and FeTiH; and the subsequent rise is the region of FeTiH and $FeTiH_2$. The effect of increased temperature is to increase the dissociation pressure, as shown in the series of isotherms in Appendix A (Fig. 1) for hydride produced from zone-refined metals. Thus for a fixed charging pressure, the driving force can be increased by operating at a lower temperature. Impurities commonly present in commercially-produced alloy can change the isotherm shape and may reduce the storage capacity of the hydride. The composition equivalent to $FeTiH_{1.95}$ can be attained with FeTi made from highly purified materials by extended contact at high pressure. For the commercial material used in the reservoir it is too time consuming to exceed a composition corresponding to $FeTiH_{\sim 1.6}$. This behavior is probably caused by high level of oxygen contamination (~3000 ppm) which tends to distort the shape of the pressure-composition isotherm. The expected operating range for the reservoir will be from $FeTiH_{0.3}$ - $FeTiH_{1.5}$. For the 879 lb of alloy used, this range will provide ~12 lb of available H_2.

RESERVOIR DESIGN

The size of the reservoir was based on the requirements previously mentioned and upon a practical operating range for the hydride. The vessel consists of a 12-in. pipe shell and two end caps welded to it. For the 0.250-in. wall thickness, the design pressure is 633 PSIG (from -20 to 200°F). A rupture disc and relief valve, in the associated piping, protect the vessel from overpressure. A diagram showing the internal arrangement of parts and a listing of some statistical data is shown in Fig. 2. All of the tubular parts are held in fixed radial position by four grid plates which are secured in axial position by three tie rods and tubular spacers (not shown). The heat exchanger consists of nine U-tubes which are uniformly spaced on two radii, as illustrated in the sectional view, and they emerge through seals in the eighteen nozzles on one end cap. Gas distribution in the bed and particle retention are achieved by means of six porous metal tubes (PMT) connected to the main gas line which is located on the vessel axis and is welded to the other end cap. The PMT are located near the center of each group of four water tubes. Thirty thermocouples (iron-Constantan) are located throughout the bed for the purpose of measuring radial and axial temperature distribution. They pass through seals in ten nozzles surrounding the main gas line, and they have a 1/16-in. o.d. sheath of type 304 stainless steel. Also located on this cap is a nozzle for the addition of alloy.

The vessel components are shown in Fig. 3. Only one of each of the three forms of U-tubes is shown, and only one PMT is shown. They are connected to the main gas line by elbow fittings attached to a radial manifold (spider) shown in Fig. 4. The grid plates were provided with a maximum amount of open area in order to ease filling of the vessel with alloy and to shorten the path for any non-radial flow of gas. A close-up view of the grid plates is shown in Fig. 5; the style at the left has central arms which support the main gas line and was used for grid plates 1 and 4. Rollers were provided at three points so that the tube bundle could be easily installed on-axis in the vessel shell. Various views of the tube bundle are shown in Figs. 6-10. All of the U-tube legs in the outer ring have 1-in. offset bends because the cap nozzles had to be kept away from the knuckle radius.

Of the 30 thermocouples (iron-Constantan) inside the reservoir, 27 measure bed temperatures and 3 measure wall temperatures. Their locations are shown in Fig. 11, and the thermocouple schedule is given in Table 1. For

the special group (G-O) of thermocouples on grid plate 4, a support bracket was added. Fig. 12 provides a view of the thermocouples in this area.

Both end caps are shown in Fig. 13; they have special seals for the U-tubes (cap at left) and the thermocouples (cap at right). Conventional swage type fittings were not used for the U-tube nozzles because if a joint had failed to make up properly, dismantling of the vessel would have been required. The joint design is based on a deformable plastic ferrule which is confined in order to prevent extrusion and is axially loaded to maintain a compressive force. A drawing of the U-tube joint is shown in Fig. 14A. The three thermocouples passing through each nozzle are sealed by a joint based on the same principles; this design is shown in Fig. 14B. The cap at the right has an access nozzle (for alloy addition) having an O-ring joint, and it also has the central nozzle for the main gas line. Both caps have a skirt ring which is used for supporting the reservoir on its stand as shown in Fig. 15.

The water supply for each U-tube is controlled by a shut-off valve at its inlet end and a throttling valve at its outlet end. Thermocouples are located in the water inlet line and in each of the outlet lines after the throttling valve. A close-up view of the inlet valve manifold is shown in Fig. 16; the outlet valve manifold is similarly arranged. Each end of the U-tubes is provided with a connector having an internal seal which is expanded against the inside of the tubing by tightening the external nut. Fig. 17 shows the U-tube arrangement and the water flow pattern.

Detail drawings of the reservoir construction are provided in Appendices B and C.

ALLOY PREPARATION AND ACTIVATION

The alloy used for this reservoir was prepared from commercial-grade Fe and Ti, and the purchased ingots were processed at BNL. Four of the seven batches produced were selected for use based on the behavior of hydrided samples. The last two batches used contained 1 and 2% Mn, in place of Fe, because tests showed that it compensated to some extent for the high oxygen content. From each batch of screened material the fractions ranging in size from 4 to 100 mesh were mixed together; 85% of the alloy used was between 4 and 20 mesh in size. Fig. 18 is a photograph of a representative sample of the alloy used. Analytical and size/weight data for this material is listed in Tables 2 and 3. With the vessel suspended in a near vertical position 879 lb of alloy was poured in to the level of grid plate 4. The remaining volume (8.2%) was left for expansion of the bed during hydriding.

In the process of converting FeTi alloy to the hydride, conditioning or activation is required before a good reaction rate is obtained. This step was performed by external electrical heating of the reservoir, outgassing at ~600°F, contacting with H_2 at a pressure of ~20 PSIA, cooling to room temperature, and then increasing the H_2 pressure to 550 PSIA. The reservoir was occasionally oscillated about its longitudinal axis in order to avoid local compaction. During activation the surface becomes cleaned and microfissures develop, thus increasing the surface area. When 5 lb of H_2 had reacted with the alloy, the bed was dehydrided and pumped down to a very low H_2 level, then the reservoir was repressurized to 550 PSIA. By the end of two weeks, 14 lb of H_2 had reacted and produced material equivalent to $FeTiH_{1.64}$. The hydrogen used was of commercial purity and was supplied in previously cleaned cylinders, thereby maintaining its purity at 99.99%.

ASSOCIATED EQUIPMENT

The various items of equipment required for the hydrogen distribution and water lines connected to the reservoir are shown on the equipment diagram in Fig. 19. Most of this equipment was supplied by BNL along with the reservoir and compressor. The main gas or supply line (darkened) contains an emergency shut-off valve at the vessel, a filter (made from the same PMT material) and two valves. It is assumed that there is a pressure regulator in the fuel-cell stack inlet line. Provisions are included for manual and automatic pressure relief, for indicating the pressure, and for sounding an alarm when the pressure reaches the chosen set point. The function of the relief valve is to minimize the loss of H_2 and to prevent the entry of air. The rupture disc is a reverse buckling type with the pressure loading on the convex side (metal is under compression). Under excess pressure a reversal in shape occurs and the disc is slit open by the four knife blades at the outlet side of the assembly. Any condensate forming in the vent line to the roof will collect in the trap and not block the release of H_2. In the water supply system a high-temperature control is provided so that if the water temperature becomes excessive, the solenoid valve will close and thereby prevent overpressurizing the vessel due to the increase in dissociation pressure. The air line connection is for blowing the water out of the outdoor lines and U-tubes when freezing is possible. Fig. 20 shows the outdoor piping assembly for the distribution of H_2.

OPERATION

The behavior of the reservoir is dependent upon the bed temperature, the H_2 pressure and the thermal load. Heat must be removed during hydriding and it must be supplied during dehydriding. Depending upon the hydrogen flow rate, a water flow rate of up to 5 GPM will be satisfactory; a rate resulting in a Δt of 5-10°F is suitable. Prior to the start of an operation, all valve settings should be checked for their proper position. The emergency shut-off valve at the reservoir should always be open unless a procedure calls for it to be closed. If this valve is to be closed, it should be properly tagged and the proper personnel should be notified.

Prior to operating the reservoir for the first time, the manifold water valves should be reset. The outlet valves should be adjusted for equal flow rates, with the inlet valves fully opened. Overall flow control is accomplished with the valve downstream from the rotameter. The inlet valves are provided so that water flow to individual tubes can be stopped if desired. When H_2 is to be discharged from the bed, ample heat must be supplied by the water flowing through the U-tubes to maintain the bed temperature above 32°F. If not enough heat is provided there is a risk of rupturing the tubes if the water freezes. The flow of hot water should be started when hydrogen discharge is started. Likewise during charging the flow of H_2 and cold water should be started at the same time. If very rapid charging of the depleted bed is to be done, the bed can be precooled. Changes in overall bed temperature will not occur rapidly because of the sensible heat of the bed.

Operation of the compressor is described in the manual supplied with the compressor. Its performance was not checked at BNL, but it was tested at the factory.

SAFETY AND PRECAUTIONARY MEASURES

These measures are concerned with the leakage of H_2, the build-up of excess pressure, and the freezing of water in the U-tubes. Operating personnel must be alerted to these potential dangers. Excess pressure can be handled by the pressure relief system, provided the emergency shut-off valve (connected to the reservoir) is open. Excess pressure can be vented manually if there is time to do so. The excess flow valve on the discharge side of the safety head is normally vented to the atmosphere so that the rupture disc can function properly. If the disc is ruptured this valve will close and the system pressure will be indicated on the adjacent gage.

Because the bed does not behave homogeneously, the temperature should be periodically scanned (or an alarm point can be set on the temperature recorder) for any approach to 32°F so that corrective action can be taken. During cold weather it is preferable to blow the lines free of water during non-operating periods. A related problem is that of thermally-induced water expansion between closed valves. None of the inlet valves should be closed when the flow control valve is closed.

The main precautionary measure is to avoid contaminating the reservoir with air or impure H_2. Contamination will reduce the reservoir performance and may require reactivation of the bed. Transfer lines can be evacuated and back-filled with H_2 and the reservoir should be kept well above atmospheric pressure.

MAINTENANCE

No routine maintenance is required other than checking for H_2 leaks. The bed will require reactivation only if it becomes contaminated. The filter in the manifold is removable if cleaning becomes necessary. Instructions for replacing a rupture disc are included with the spare discs. The disc is a reverse buckling style; so it must be installed with pressure loading on the convex side.

LIST OF FIGURE CAPTIONS

Fig.	Caption
1	Pressure-Composition Relationship at 63°F for the Fe-Ti-H System.
2	Diagram Showing Internal Components of Reservoir, Accompanied by Some Reservoir Statistics.
3	Vessel Components of the Hydrogen Reservoir.
4	Main Gas Line with Radial Arms for the PMT.
5	Typical Grid Plates.
6	Oblique End View of U-Tubes, PMT and Main Gas Line.
7	Oblique End View of U-Tube Ends and PMT Spider.
8	Side View of Tube Bundle.
9	End View of U-Bends and PMT Ends.
10	End View of U-Tube Ends and Spider.
11	Thermocouple Locations.
12	Special Group of Thermocouples on Grid Plate 4.
13	Vessel End Caps.
14A	Joint Design of a U-Tube Nozzle.
14B	Joint Design of a Thermocouple Nozzle.
15	Hydrogen Reservoir Ready for Operation.
16	Inlet-Valve Manifold and Connecting Lines.

Fig.	Caption
17	U-Tube Arrangement and Water Flow Pattern.
18	Appearance of the Granular Alloy Used.
19	Equipment Diagram for Hydrogen-Energy Storage System, Public Service Electric & Gas Co. of N. J.
20	Outdoor Piping Assembly.

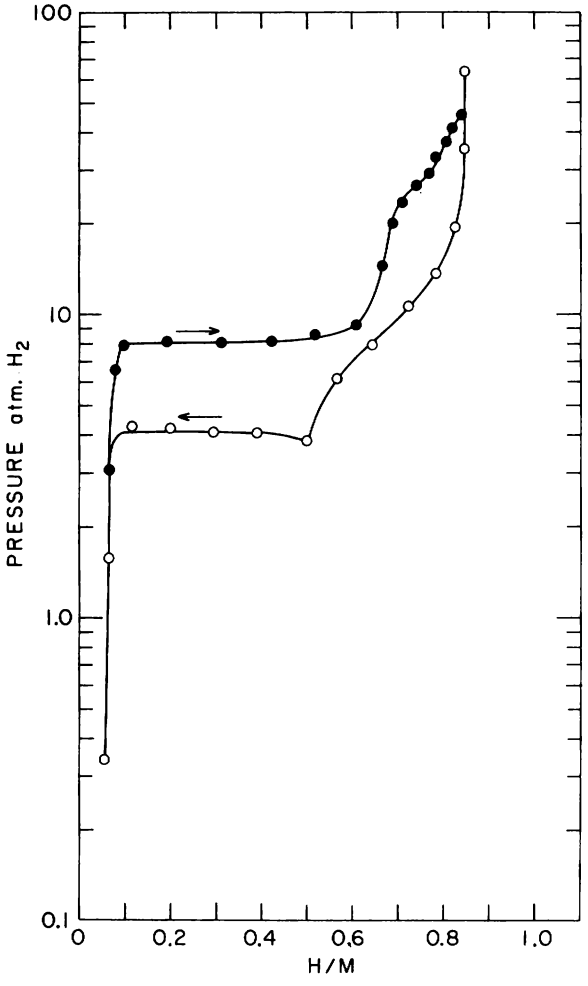

Figure 1. Pressure-Composition Relationship at 63°F for the FeTi-H System.

HYDROGEN RESERVOIR

CONTAINING
14 LB HYDROGEN WITH 879 LB IRON TITANIUM ALLOY
GROSS WEIGHT 1241 LB
REACTION: $FeTiH_{0.2} \leftrightarrow FeTiH_{1.5}$ MIN. RANGE, APPROX. 12 LB H_2 AVAILABLE

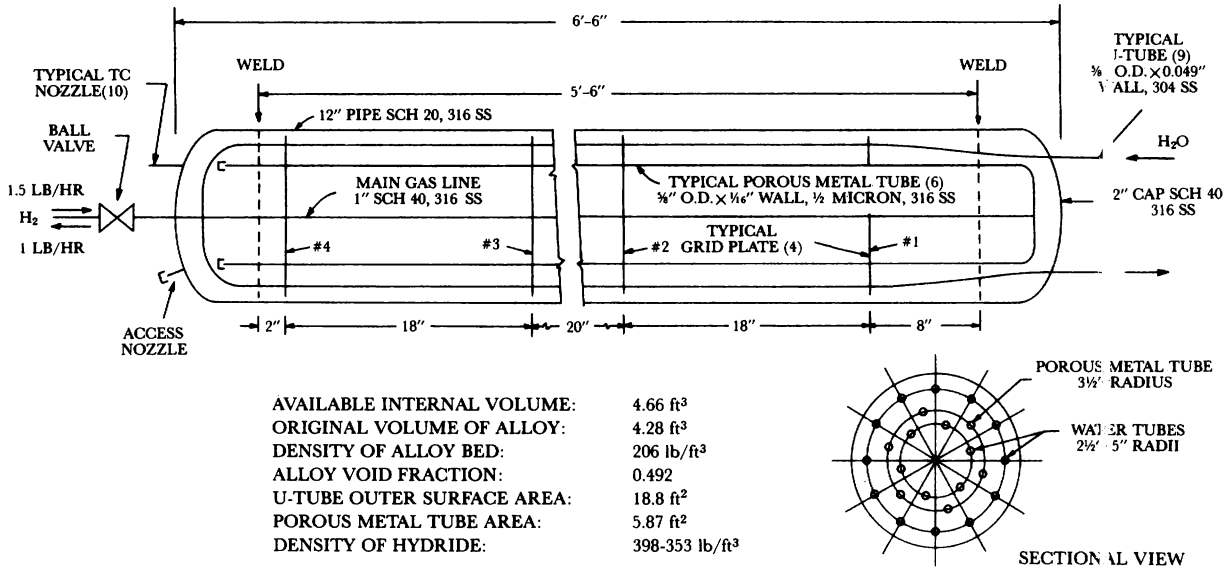

AVAILABLE INTERNAL VOLUME:	4.66 ft^3
ORIGINAL VOLUME OF ALLOY:	4.28 ft^3
DENSITY OF ALLOY BED:	206 lb/ft^3
ALLOY VOID FRACTION:	0.492
U-TUBE OUTER SURFACE AREA:	18.8 ft^2
POROUS METAL TUBE AREA:	5.87 ft^2
DENSITY OF HYDRIDE:	398-353 lb/ft^3

Figure 2. Diagram Showing Internal Components of Reservoir, Accompanied by Some Reservoir Statistics.

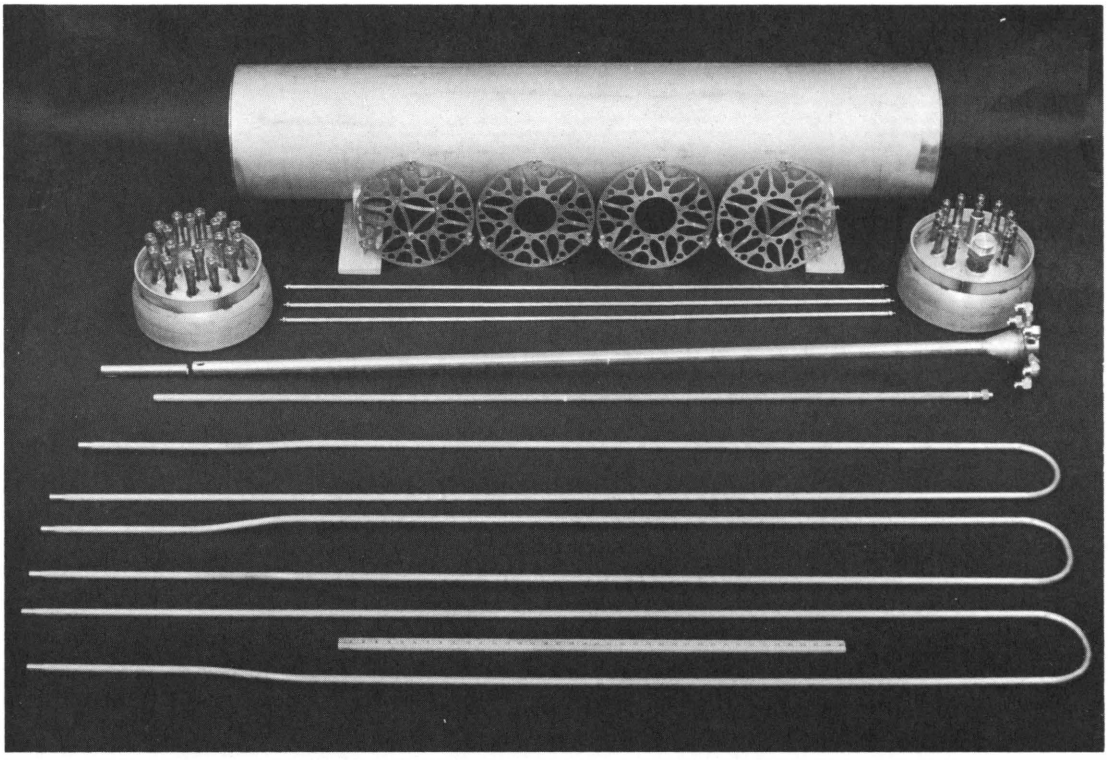

Figure 3. Vessel Components of the Hydrogen Reservoir.

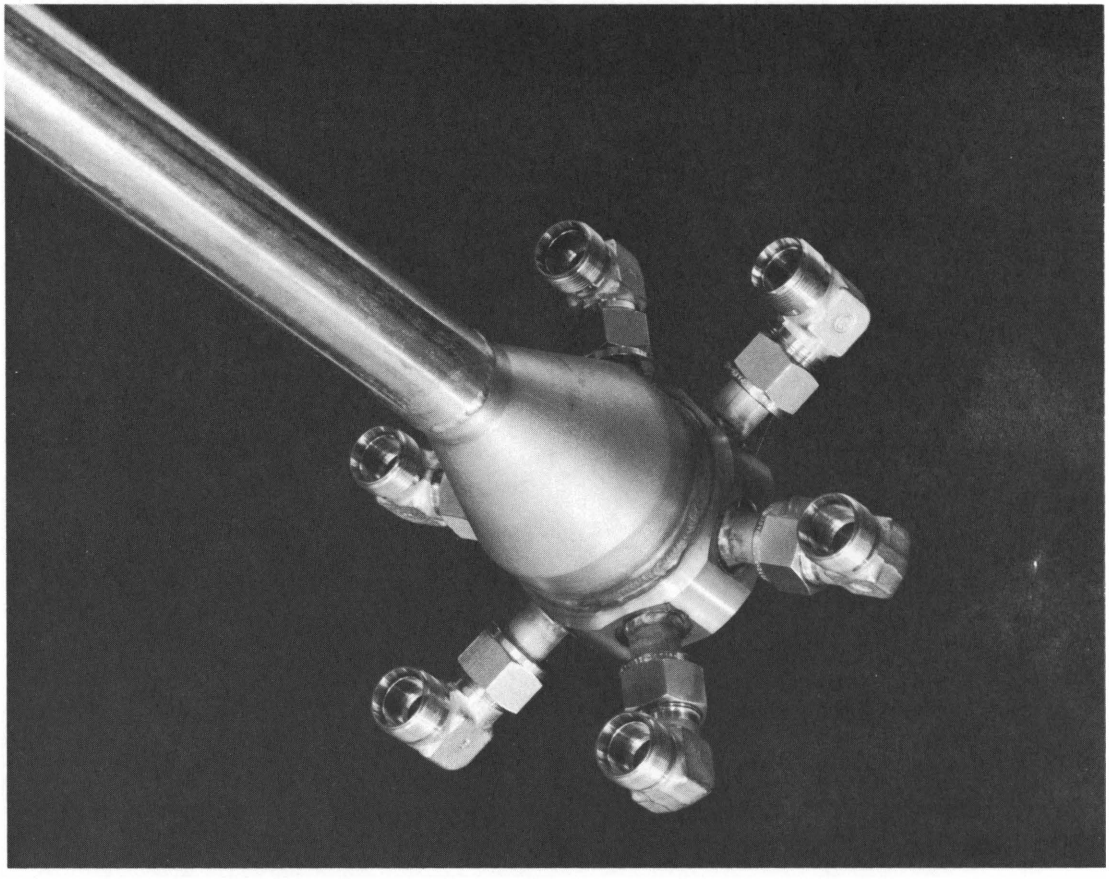

Figure 4. Main Gas Line with Radial Arms for the PMT.

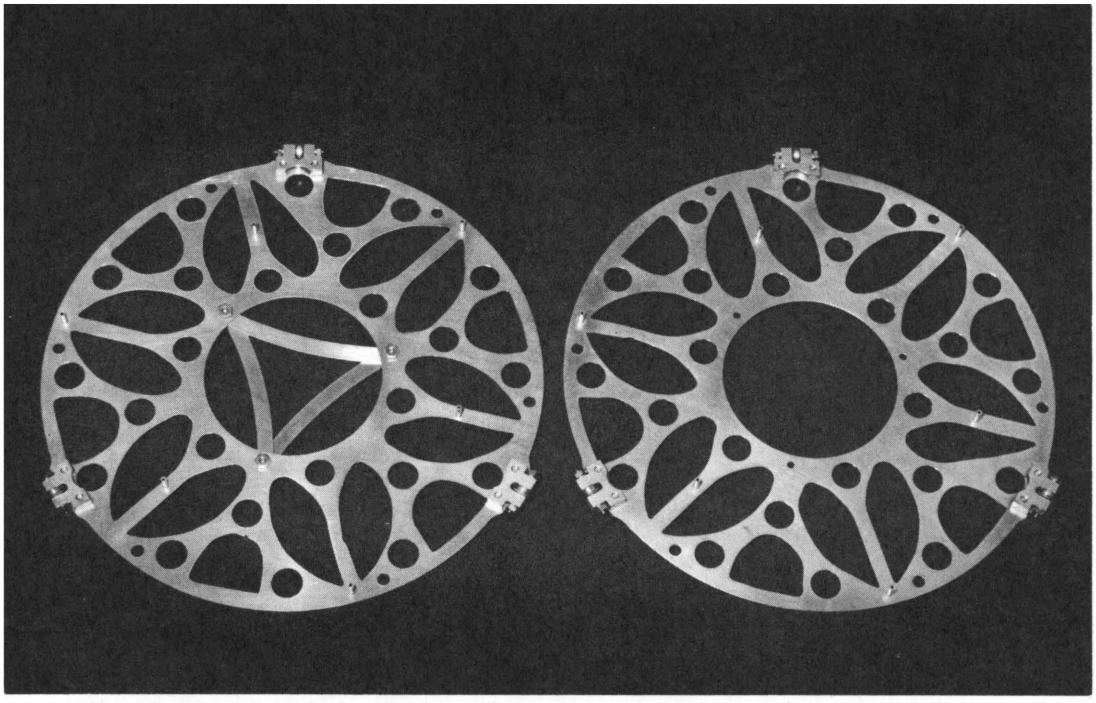

Figure 5. Typical Grid Plates.

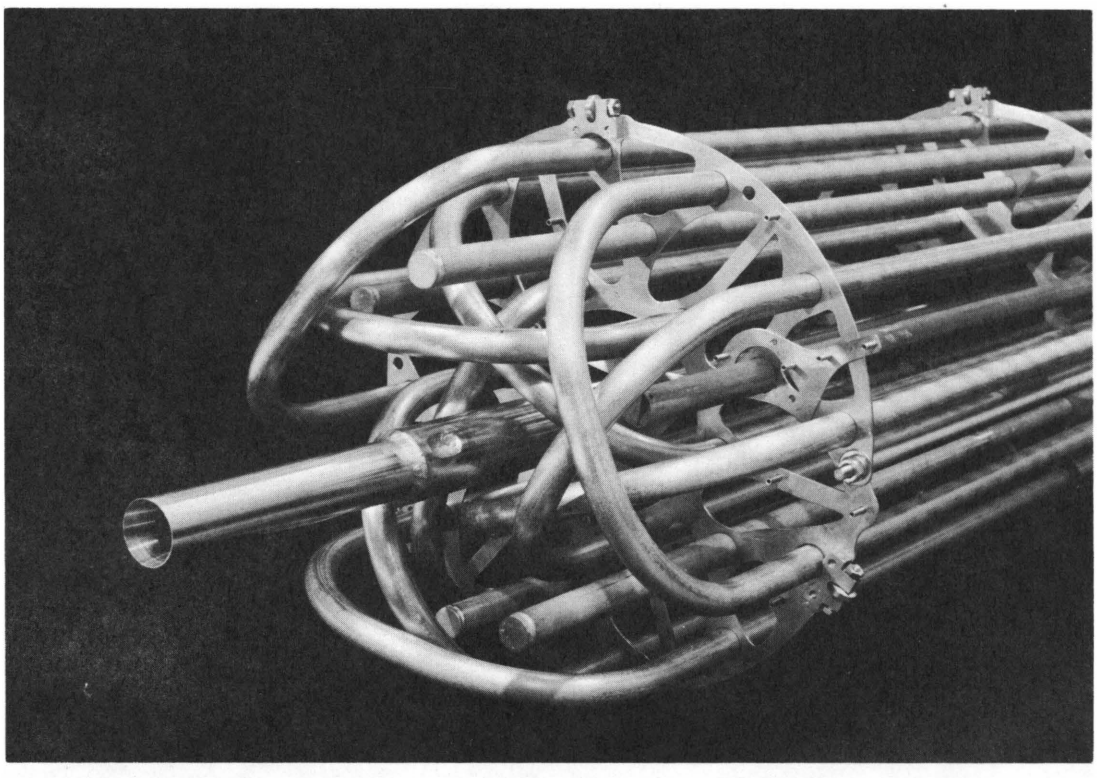

Figure 6. Oblique End View of U-Tubes, PMT and Main Gas Line.

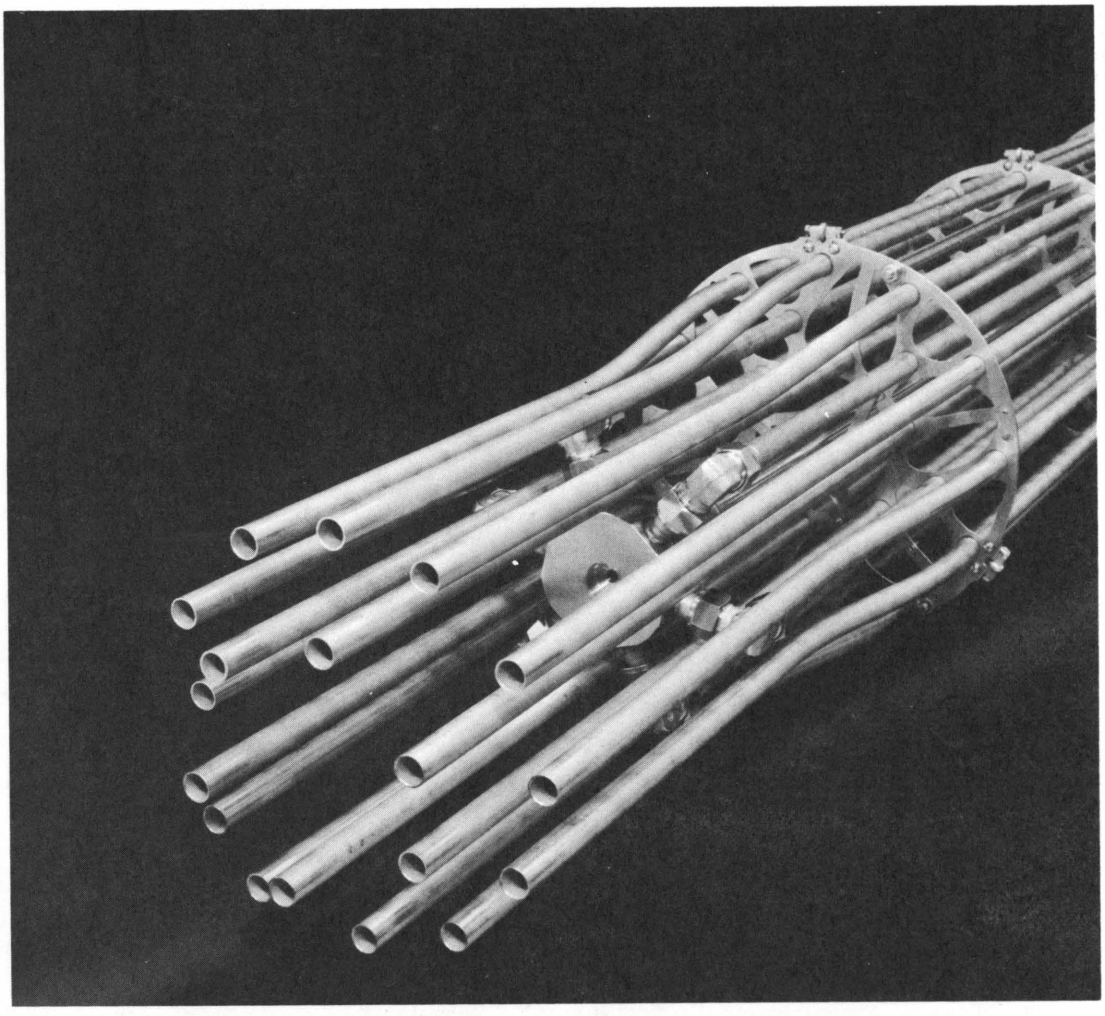

Figure 7. Oblique End View of U-Tube Ends and PMT Spider.

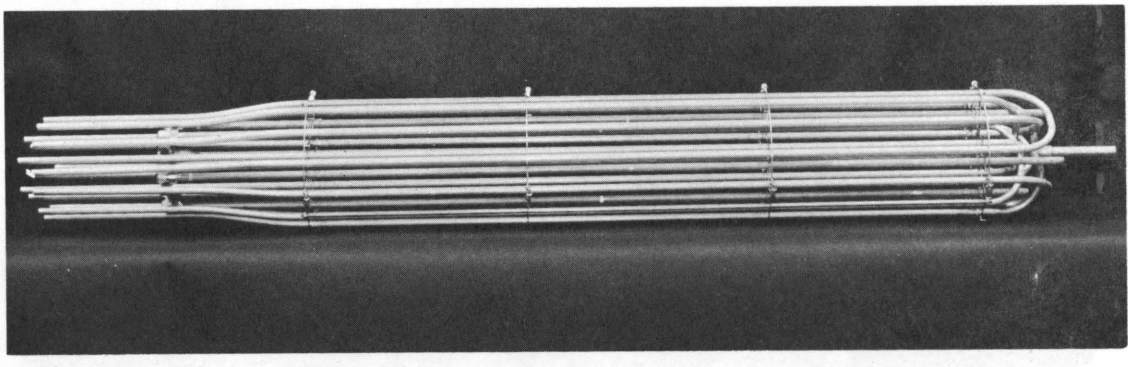

Figure 8. Side View of Tube Bundle.

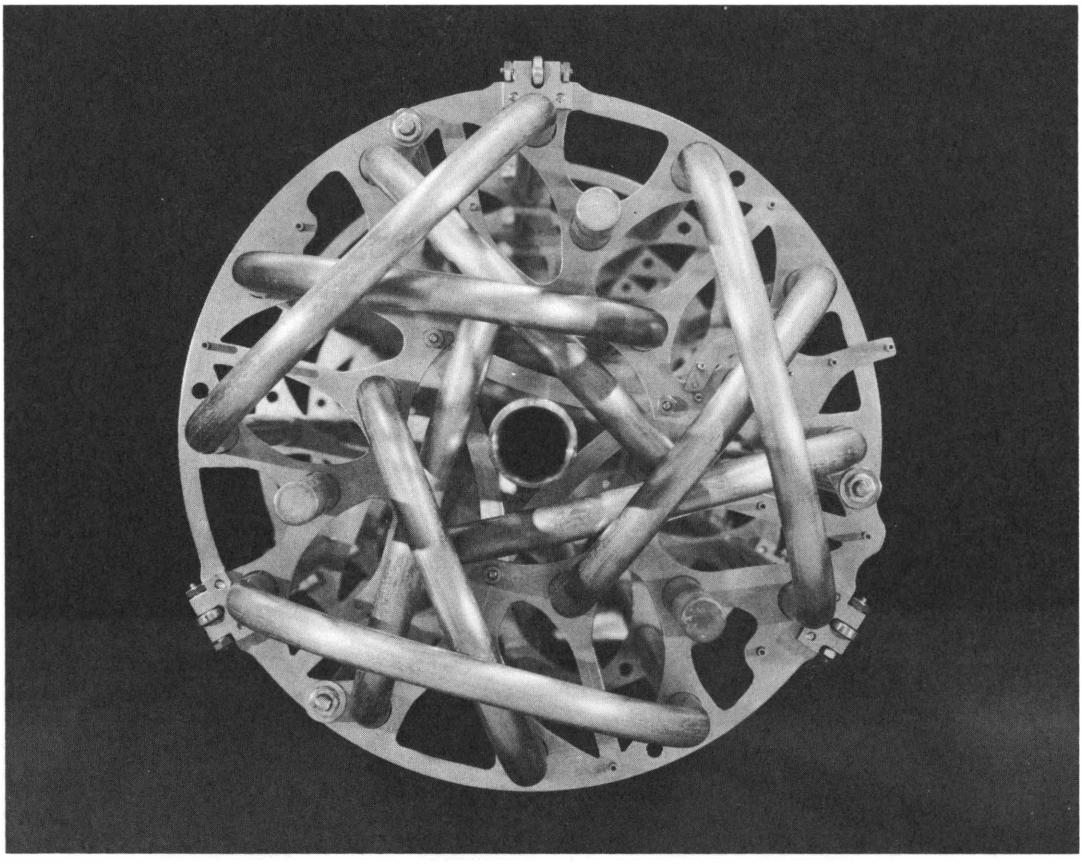

Figure 9. End View of U-Bends and PMT Ends.

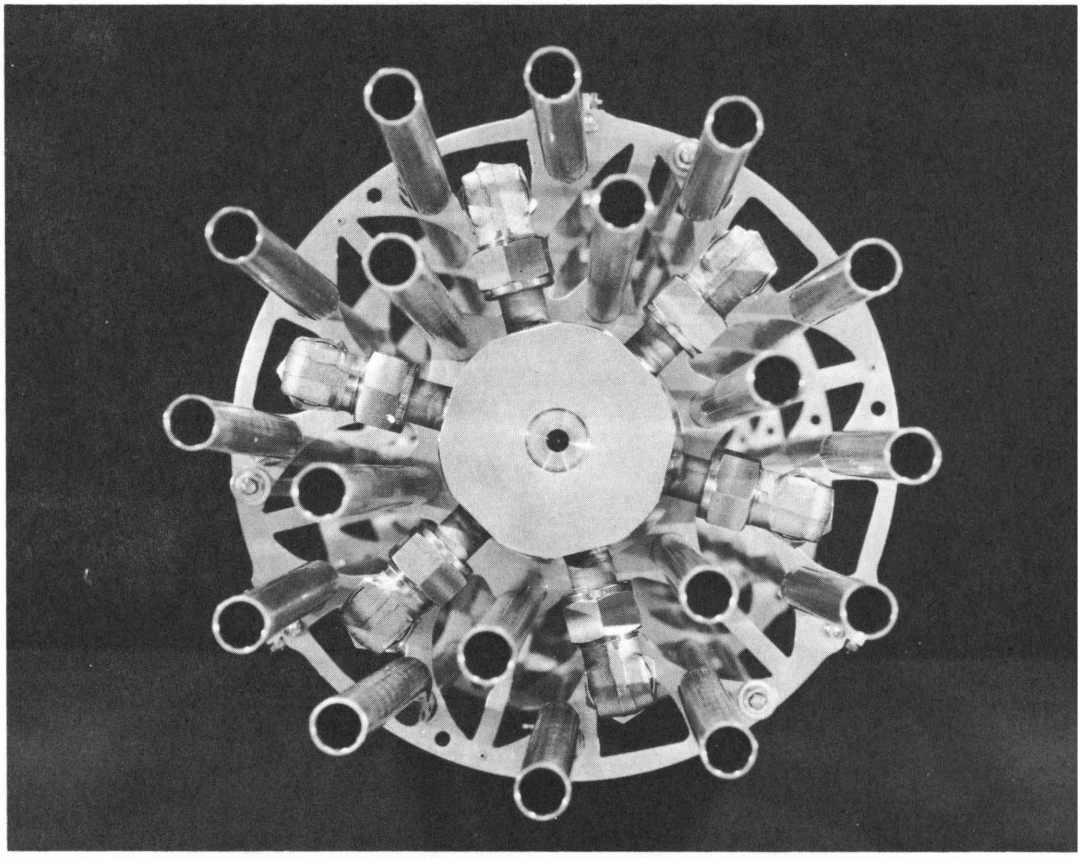

Figure 10. End View of U-Tube Ends and Spider.

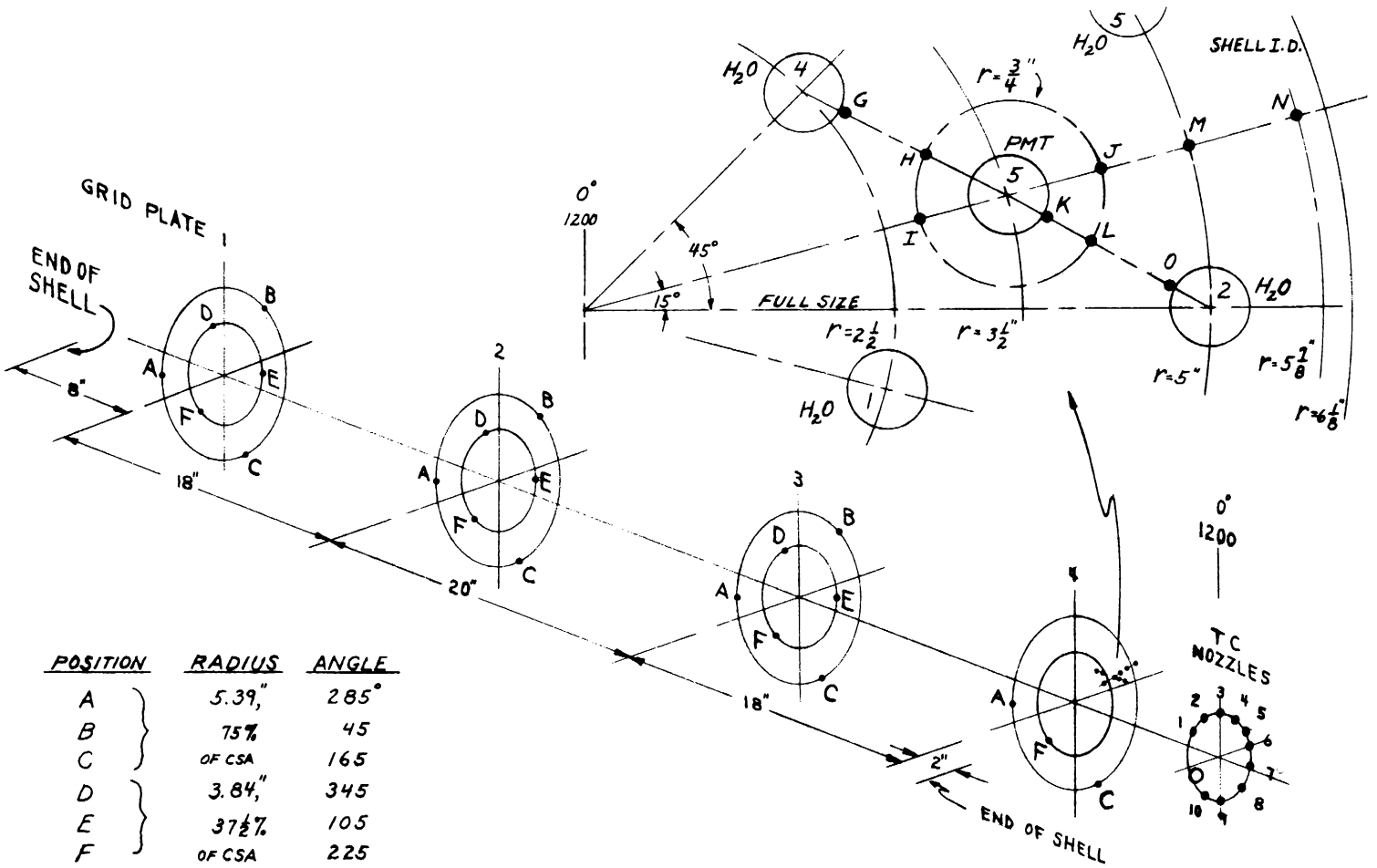

Figure 11. Thermocouple Locations.

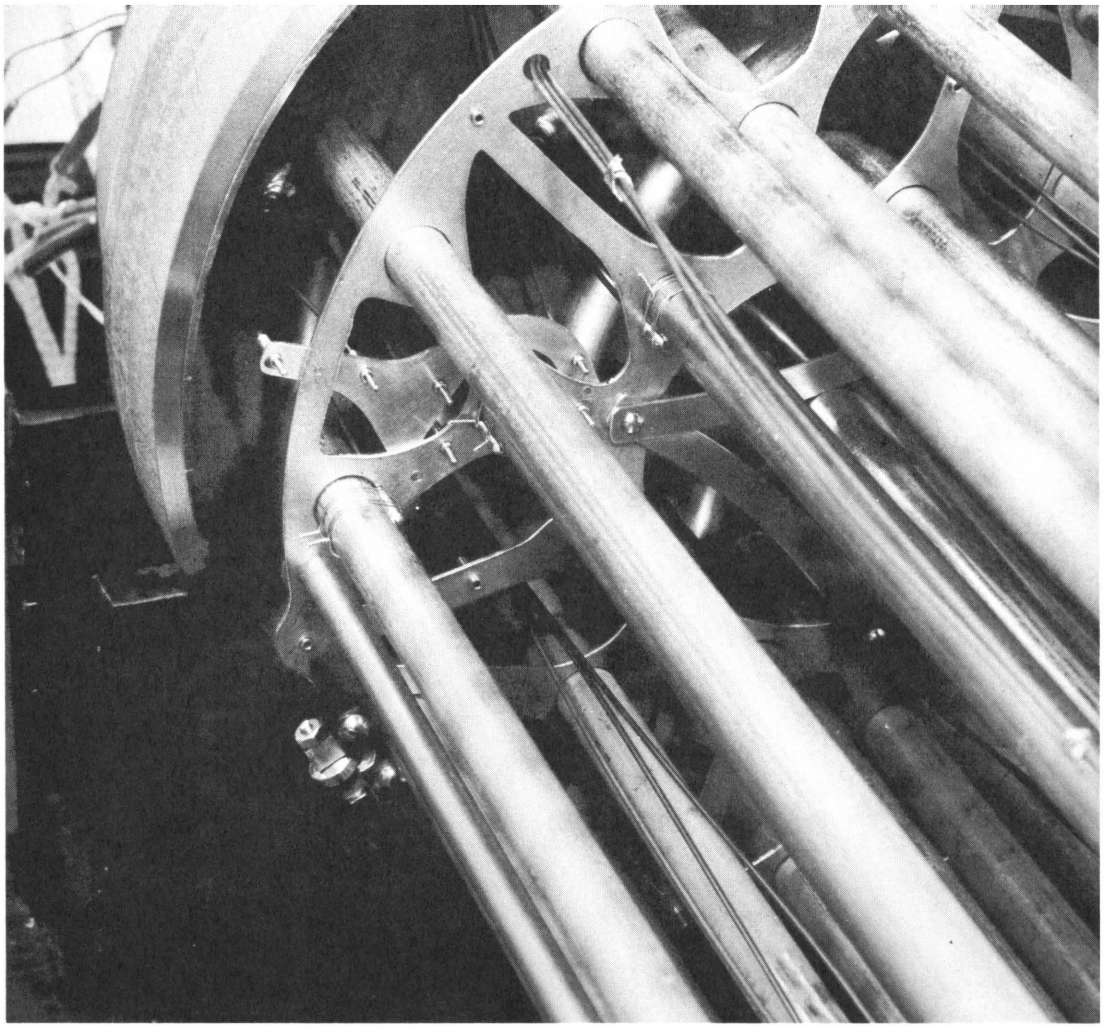

Figure 12. Special Group of Thermocouples on Grid Plate 4.

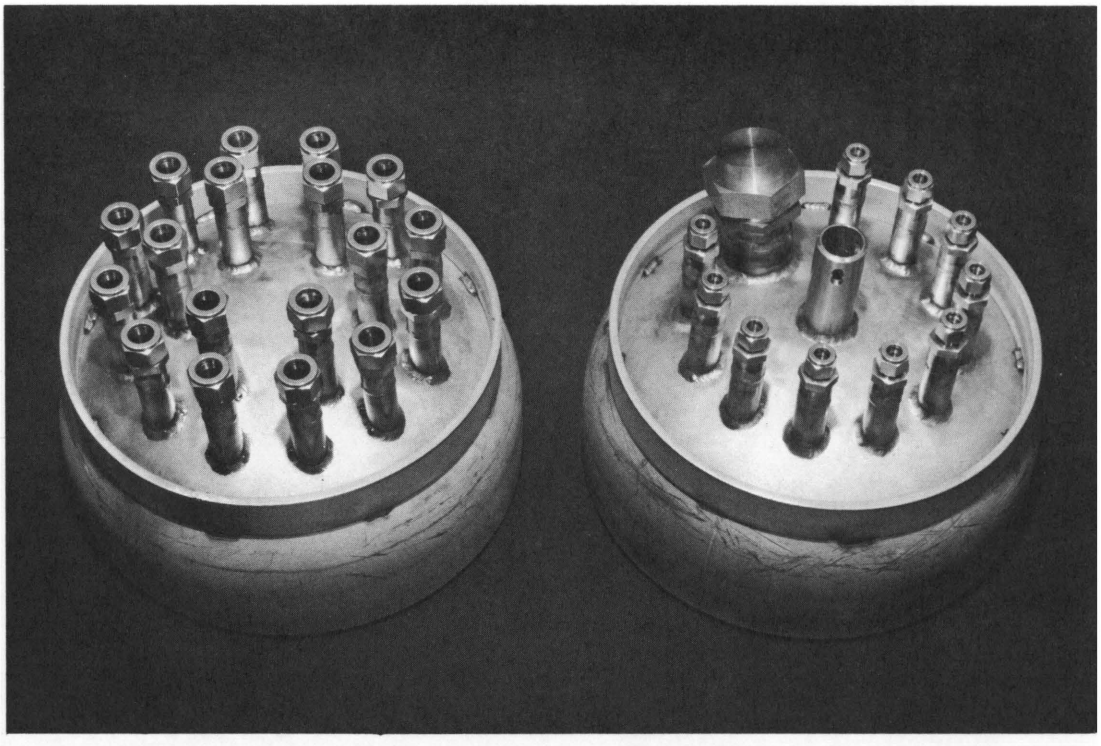

Figure 13. Vessel End Caps.

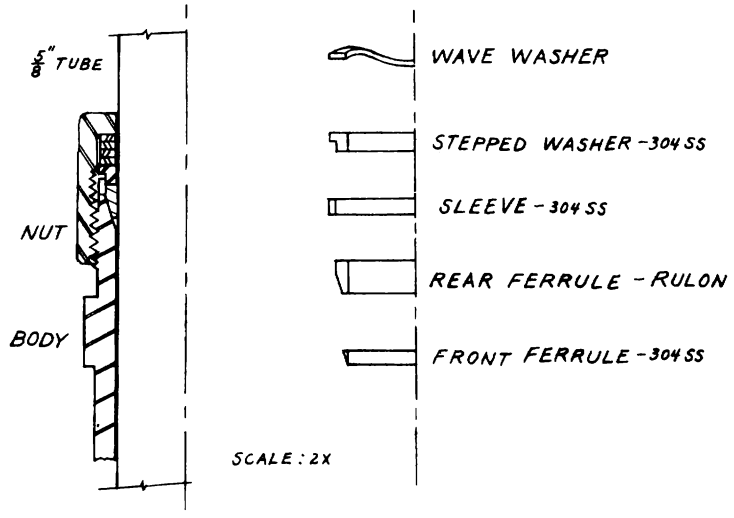

Figure 14A. Joint Design of a U-Tube Nozzle.

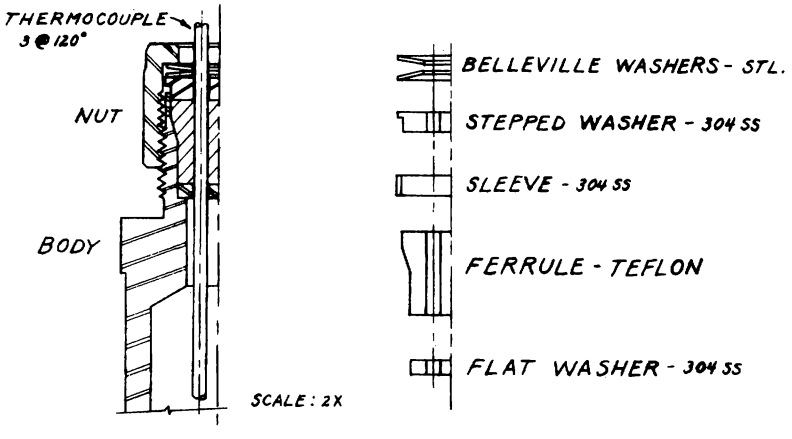

Figure 14B. Joint Design of a Thermocouple Nozzle.

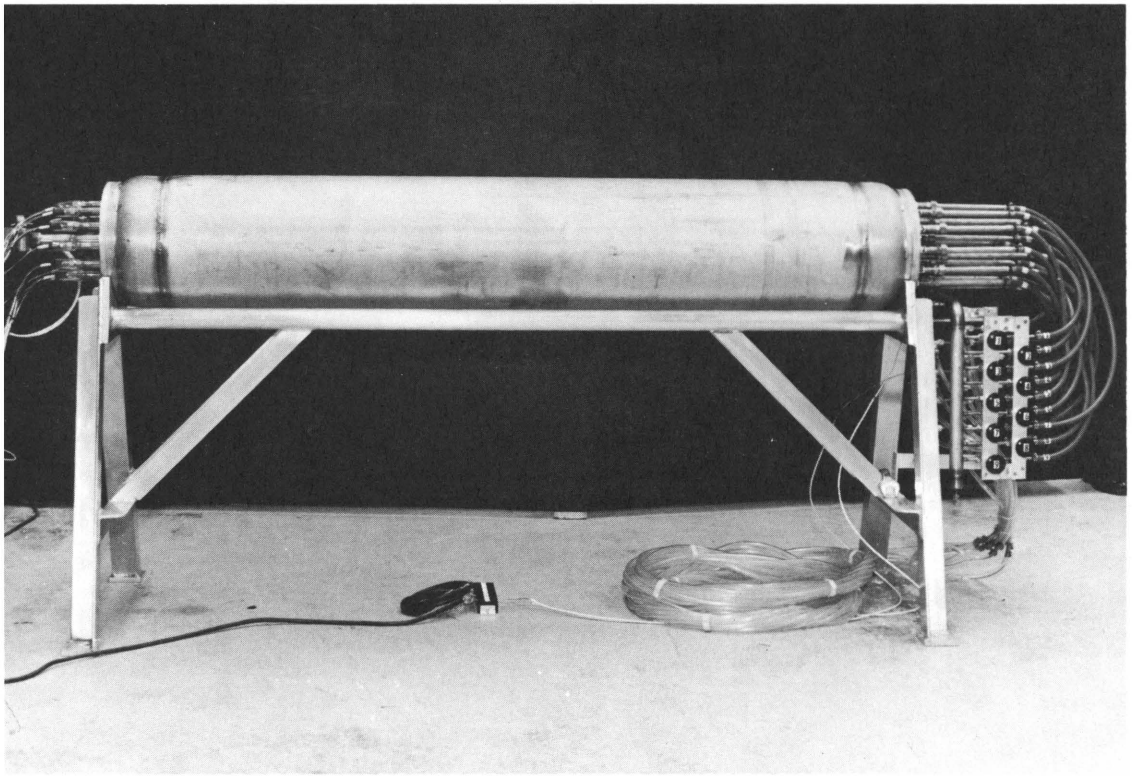

Figure 15. Hydrogen Reservoir Ready for Operation.

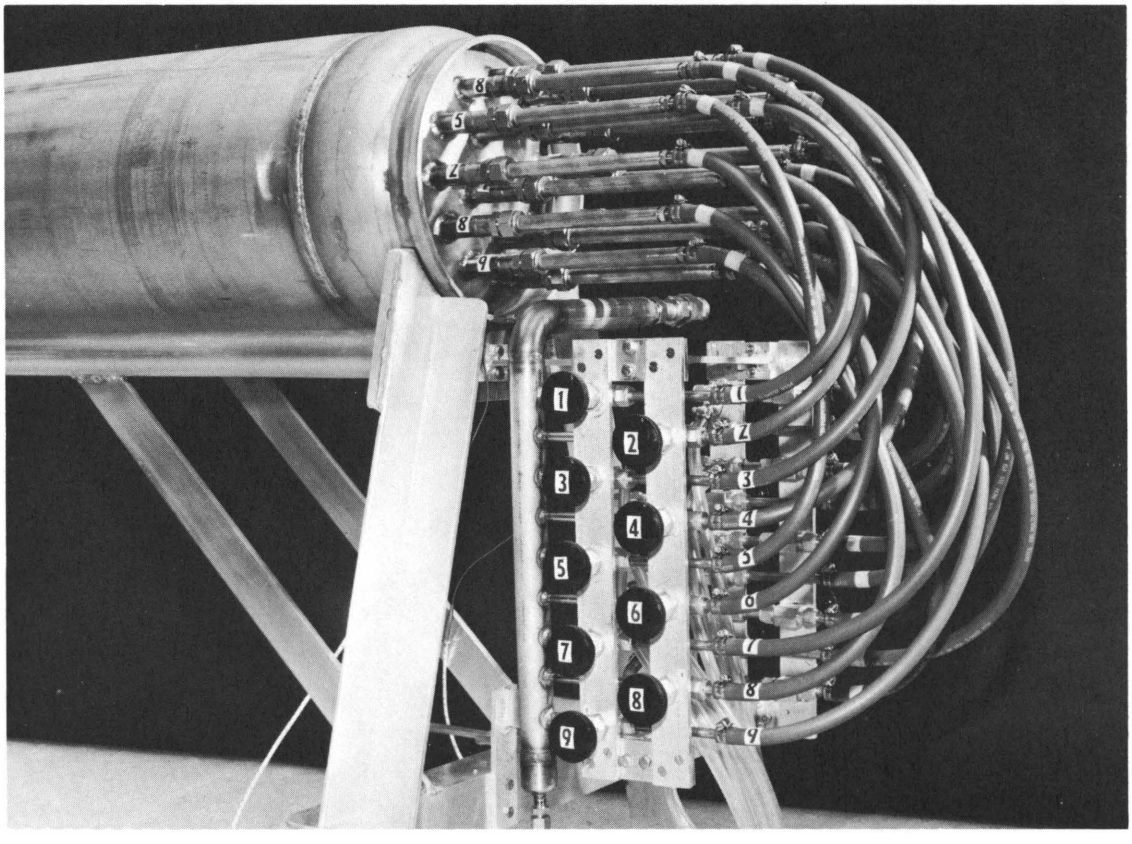

Figure 16. Inlet-Valve Manifold and Connecting Lines.

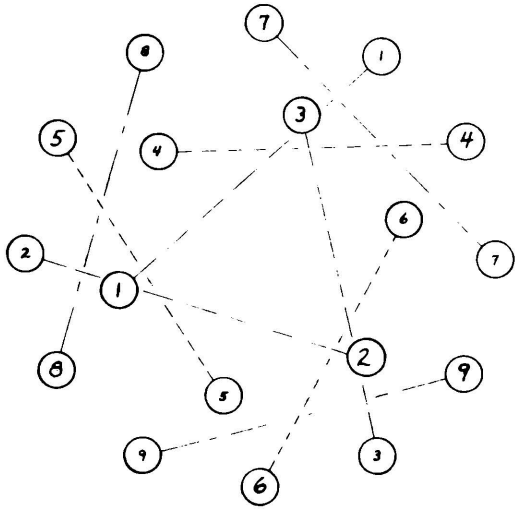

Figure 17. U-Tube Arrangement and Water Flow Pattern.

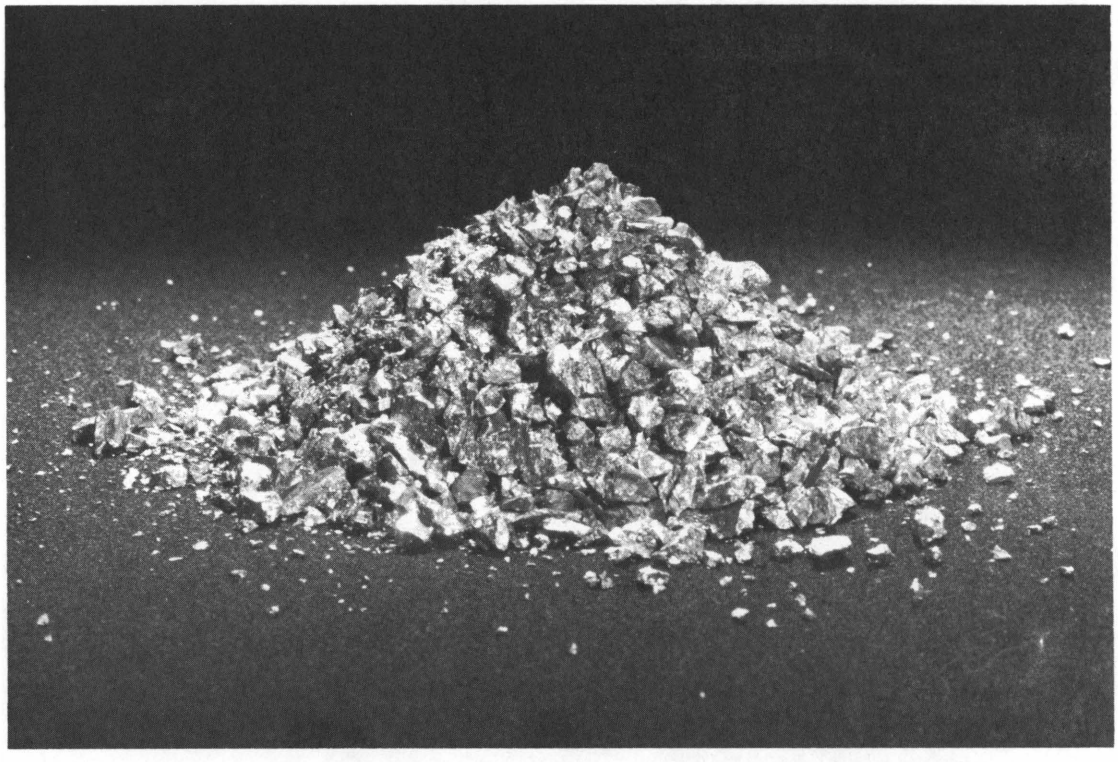

Figure 18. Appearance of the Grannular Alloy Used.

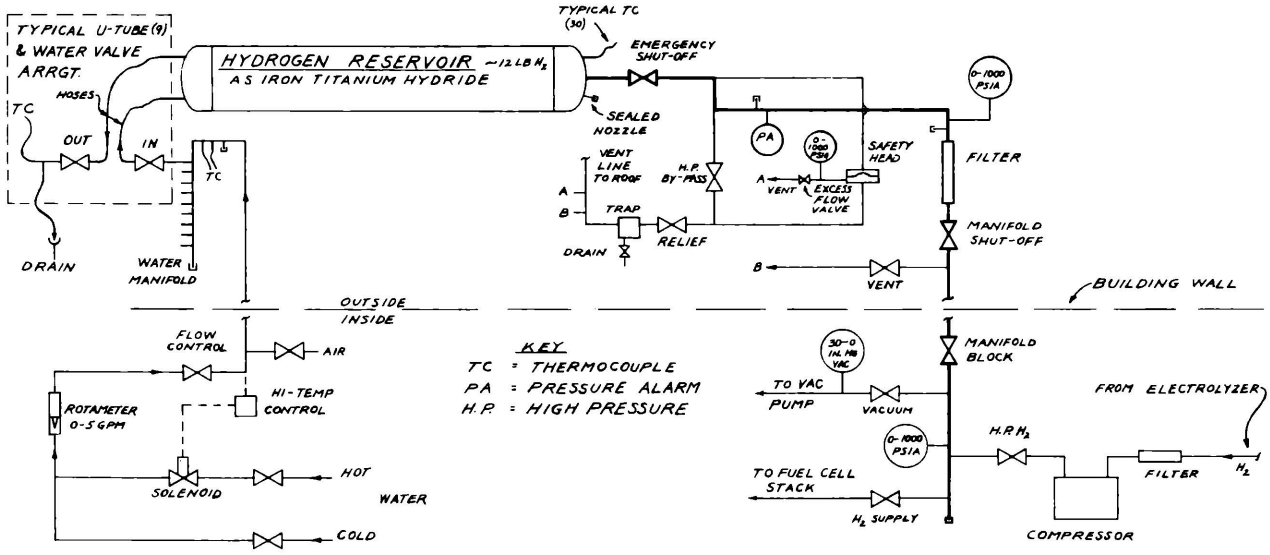

Figure 19. Equipment Diagram for Hydrogen-Energy Storage System, Public Service Electric & Gas Co. of N.J.

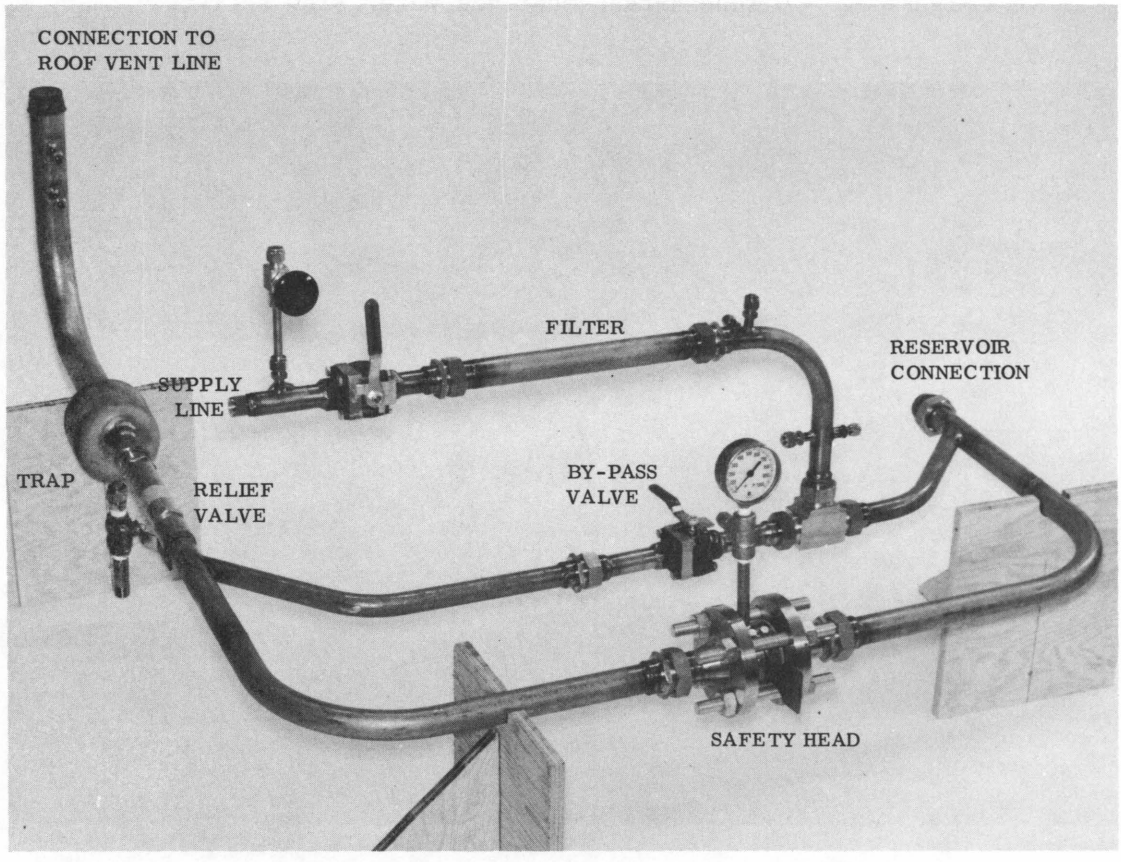

Figure 20. Outdoor Piping Assembly.

LIST OF TABLES

TABLE 1

THERMOCOUPLE SCHEDULE

TC	NOZZLE	GRID PLATE	POSITION
1	1	3	A
2	1	2	A
3	1	1	A
4	2	3	D
5	2	2	D
6	2	1	D
7	3	3	B
8	3	2	B
9	3	1	B
10	4	4	G(a)
11	4	4	H
12	4	4	I
13	5	4	J
14	5	4	K(b)
15	5	4	L
16	6	4	M
17	6	4	N
18	6	4	O(c)
19	7	3	E
20	7	2	E
21	7	1	E
22	8	3	C
23	8	2	C
24	8	1	C
25	9	3	F
26	9	2	F d)
27	9	1	F d)
28	10	4	A
29	10	4	C
30	10	4	F

(a) In contact with H_2O tube 4.
(b) In contact with PMT 5.
(c) In contact with H_2O tube 2.
(d) Broke off at nozzle because of improper support when the reservoir was oscillated during activation of the alloy.

TABLE 2

FeTi ALLOY ANALYSES

Wt %

BATCH NO.	1	2	3	4
Fe	52.7	51.1	51.3	50.7
Ti	46.0	47.0	46.2	45.5
Mn	-	-	1	2
O	0.29	0.39	0.27	0.31
C	0.015	<0.01	<0.01	<0.01

TABLE 3

PARTICLE SIZE DISTRIBUTION OF COMPOSITE FeTi SAMPLE

WEIGHT		MESH SIZE	
Grams	%	+	-
1147	38.0	7	4
557	18.5	10	7
853	28.3	20	10
208	6.9	40	20
185	6.1	60	40
33	1.1	80	60
32	1.1	100	80

TABLE 4

VARIOUS VALUES RELATED TO PRESSURE RELIEF

	PSIG	PSIA
Vessel Design Pressure	633	64[illegible]
Rupture Disc Rating (a)	618	63[illegible]
Minimum Bursting Pressure	605	62[illegible]
Maximum Operating Pressure (b)	545	56[illegible]
Relief Valve Cracking Pressure (c)	518	53[illegible]
Relief Valve Opening Pressure (d)	545	56[illegible]

(a) ±2%
(b) 90% of the minimum bursting pressure.
(c) measured value after adjustment.
(d) calculated as 1.05 × cracking pressure.

APPENDIX A

[Reprinted from Inorganic Chemistry, 13, 218 (1974).]

Formation and Properties of Iron Titanium Hydride[1]

J. J. REILLY* and R. H. WISWALL, Jr.

Received March 1, 1973

The intermetallic compound FeTi reacts directly with hydrogen to form, in succession, hydrides of the approximate compositions FeTiH and $FeTiH_2$. The composition limits have been determined and are diagrammed. Both hydrides have dissociation pressures of over 1 atm at 0°, unlike the very stable TiH_2. The relative partial molar enthalpies of hydrogen have the rather low values of −3.36 kcal/g-atom of hydrogen in the lower hydride and −3.70 to −4.03 in the higher; the properties of the latter vary with the hydrogen content. Pronounced hysteresis effects are observed, the absorption isotherms of pressure *vs.* composition frequently being several atmospheres higher, at a given composition, than the desorption isotherms. The lower hydride, FeTiH, has tetragonal symmetry and a density of 5.88 g/cm³. The higher hydride has a cubic structure and a density of 5.47 g/cm³ ($FeTiH_{1.93}$). The hydriding behavior is quite sensitive to the composition of the solid phase. If Ti is in slight excess over the equiatomic proportion, the pressure–composition isotherms no longer exhibit the plateaus and inflections characteristic of the appearance of new phases.

Iron and titanium form two known stable intermetallic compounds, FeTi and Fe_2Ti.[2] It is also generally accepted that a third compound, $FeTi_2$, exists above 1000°, decomposing to FeTi and Ti below that temperature.[3] We have briefly noted previously[4] that one of these compounds, FeTi, will react directly with hydrogen to form an easily decomposed hydride which may be useful as a hydrogen storage medium. Our purpose here is to discuss the Fe-Ti-H system in some detail with particular emphasis on the reaction of FeTi with hydrogen and the formation and properties of two ternary hydrides, $FeTiH_{\sim 1}$ and $FeTiH_{\sim 2}$.

Experimental Section

The Fe–Ti alloys were prepared from zone-refined Fe and Ti in an arc furnace under an argon atmosphere, although it should be noted that no significant differences were observed when commercial grade Fe and Ti were substituted for the zone-refined starting material. Initially we had prepared the alloys in an induction furnace; however, it appeared that the resulting products were contaminated by the alumina crucible material, which had an inhibiting effect upon their reaction with hydrogen. Contamination of iron titanium alloys by alumina crucibles has been noted previously.[2] All the alloys were quite brittle and all samples were crushed to pass through a 10-mesh screen. It was not necessary to carry out the crushing step in an inert atmosphere. The samples, weighing ~10 g, were introduced into a high-pressure hydriding reactor, the construction of which has been previously discussed in detail.[5]

Our procedure for hydriding metals which form unstable hydrides, as in this instance, has also been described,[6] and only a brief synopsis will be given here. The reactor was loaded with the granular alloy samples, sealed, evacuated, and then heated to 400–450° while outgassing continuously. Upon reaching the cited temperature range, hydrogen was admitted to the reactor until the pressure was ~7 atm. There was usually a slight drop in hydrogen pressure at this point due to some solution of hydrogen in the metal phase. After ~30 min the reactor was evacuated and cooled to room temperature at which point H_2 was admitted to the reactor until the pressure was ~65 atm. Usually the metal–hydrogen reaction proceeded immediately with the evolution of heat. If no reaction took place over a 15-min period, the above procedure was repeated. It should be noted that if the alloy is in ingot form, rather than granular, the initiation of the reaction is somewhat more difficult and may require several such treatments. In order to obtain a highly active metal substrate, the sample was hydrided and dehydrided several times. Dehydriding was accomplished by outgassing and heating to ~200°.

The procedure for obtaining the pressure–composition isotherms presented here is essentially the same as that described previously.[5,6] Briefly, it consisted of equilibrating the metal hydride with hydrogen

(1) This work was performed under the auspices of the U. S. Atomic Energy Commission and was also partially supported by U. S. Army Mobility Equipment Research and Development Center, Ft. Belvoir, Va.

(2) R. P. Elliott, "Constitution of Binary Alloys, First Supplement," McGraw-Hill, New York, N. Y., 1965.

(3) D. H. Polonis and J. G. Parr, *Trans. AIME*, 200, 1148 (1954).

(4) (a) K. C. Hoffman, *et al.*, paper presented at the International Automotive Engineering Congress, Society of Automotive Engineers, Detroit, Jan 1969; (b) R. H. Wiswall, Jr., and J. J. Reilly, paper presented at the Intersociety Energy Conversion Engineering Conference, San Diego, Calif., Sept 1972.

(5) J. J. Reilly and R. H. Wiswall, Jr., *Inorg. Chem.*, 6, 2220 (1967).

(6) J. J. Reilly and R. H. Wiswall, Jr., *Inorg. Chem.*, 9, 1678 (1970).

at ~65 atm pressure and at a predetermined temperature. Hydrogen was then withdrawn in a measured amount from the system by venting to an evacuated reservoir of known volume. After equilibrium was reestablished as determined by no further pressure change over a period of ~3 hr, a further aliquot of hydrogen was withdrawn. This step was repeated in succession until the equilibrium pressure was below 1 atm, after which the sample was heated to >400° and any further hydrogen that evolved was measured. Finally, the sample was cooled to room temperature, removed from the reactor, and analyzed for Fe, Ti, and residual hydrogen. The analysis for the metals was accurate to ±0.5% and total cumulative error for hydrogen was estimated to be ±2.5%. Occasionally, the reverse procedure was followed in order to determine hysteresis effects. In these runs, the starting material was an alloy sample that had been activated by previous hydriding and dehydriding; and the points on the pressure *vs.* composition curve were obtained by adding successive small increments of hydrogen.

All the X-ray data were obtained using a 114.59-mm diameter Norelco powder camera (Debye–Scherrer type) using Cu Kα or Co Kα radiation.

Results and Discussion

The Fe–Ti–H system was explored between the approximate limits, by weight, of 70% Fe–30% Ti and 37% Fe–63% Ti, corresponding to the atomic proportions Fe_2Ti and $FeTi_2$. At the iron-rich end of this range no hydrogen was absorbed, but all compositions richer in Ti than Fe_2Ti did take up hydrogen to some extent. The stable intermetallic compound, FeTi, reacted readily, and a series of pressure–composition isotherms for the FeTi–H system is shown in Figure 1. The composition of the unhydrided alloy, as determined by analysis, was 53.6% Fe and 46.7% Ti. The only metal phase present should be that of FeTi, which was confirmed by an X-ray diffraction pattern taken of the sample. In the graphs the equilibrium dissociation pressure of the hydride is plotted against the hydrogen content of the alloy expressed as the ratio of hydrogen atoms to the total number of metal atoms (H/(Fe + Ti) or simply H/M). The shape of the isotherms can be interpreted as follows: on the left, where the isotherms rise steeply as the hydrogen content of solid increases, is the region of solid solution of hydrogen in the Fe-Ti metal lattice. This solid solubility region may be designated as the α phase of the FeTi–H system. As the hydrogen content of the solid is further increased, the equilibrium pressure remains constant and forms, so to speak, a plateau. The composition at which the plateau begins marks the point at which a new phase appears and also marks the maximum solubility of hydrogen in the α phase. At room temperature that composition corresponds to $FeTiH_{0.10}$ (H/M = 0.05). The new phase is the monohydride or β phase of the FeTi–H system. Both the α and β phases coexist until the solid composition corresponds to $FeTiH_{1.04}$ where the isotherms begin a steep ascent. At this point the α phase had disappeared. The dip shown in the lower temperature isotherms near this composition is discussed below. As the hydrogen content of the β phase is increased, a new phase appears, the γ or dihydride phase. Its exact point of inception is temperature dependent and is somewhat difficult to determine since the upper plateaus are narrow and the breaks in the isotherms quite gradual. The 55° isotherm shows only a vestigial plateau structure and it appears that this temperature is quite

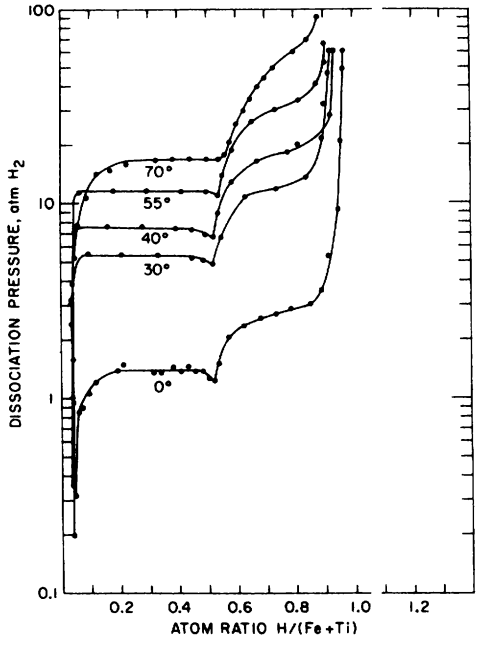

Figure 1. Pressure–composition isotherm for the FeTi–H system. The initial alloy composition was 53.6% Fe and 46.7% Ti.

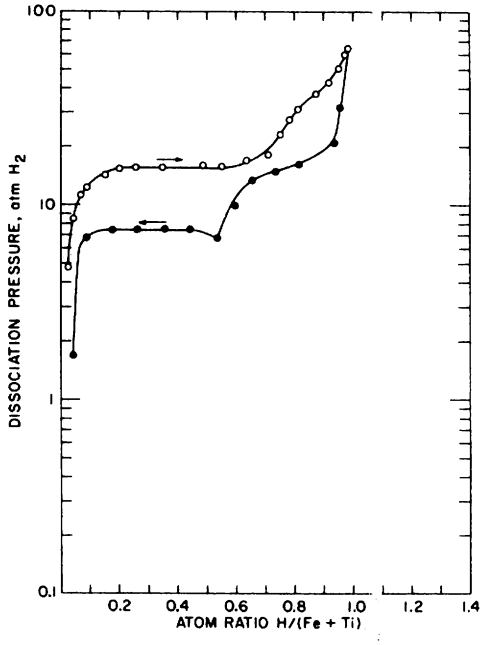

Figure 2. Hysteresis in the FeTi–H system (40°).

close to the critical temperature, above which two discrete solid hydride phases cannot coexist and the monohydride is transformed continuously into the dihydride phase. The 70° isotherm shows no evidence of a plateau in this region.

The effect of hysteresis in the FeTi–H system at 40° is illustrated in Figure 2. It is worth noting that the system almost forms two loops since hysteresis, as would be expected, is substantially reduced in the intermediate single (β) phase region. The loops do not quite close, perhaps because the

Table I. Relative Partial Molal Quantities Per Gram-Atom of Hydrogen

Compn	$(\bar{H}_H - {}^1/_2H_{H_2}°)$, kcal	$(\bar{S}_H - {}^1/_2S_{H_2}°)$, eu	$(\bar{F}_H - {}^1/_2F_{H_2}°)$, kcal	A^a	B^a
$FeTiH_{0.1}$–$FeTiH_{1.04}$	−3.36	−12.7	+0.42	−3383	+12.7612
$FeTiH_{1.20}$	−3.70	−14.4	+0.57	−3728	+14.4327
$FeTiH_{1.40}$	−3.98	−15.6	+0.65	−4020	+15.6610
$FeTiH_{1.60}$	−4.03	−15.8	+0.68	−4057	+15.9165

[a] Constants in the equation $\ln P_{atm} = (A/T) + B$.

composition range over which only the β phase is present is quite narrow. As the γ phase appears, hysteresis again increases. It is also of interest to point out that the dip occurring in the lower temperature desorption isotherms at H/M = 0.5 does not occur in the absorption isotherm. This situation appears to be analogous to that occurring in the uranium–hydrogen system below 400°, where a similar dip in the desorption isotherm was noted by Spedding, *et al.*,[7] and by Wicke and Otto.[8] Our results indicate that at higher temperatures the dip is less pronounced and finally disappears altogether in the 70° isotherm. This behavior is, again, similar to that of the uranium–hydrogen system, where Libowitz and Gibb[9] found no dips in isotherms determined at high temperatures (450°+). Wicke and Otto have suggested that the phenomenon is due to the supersaturation of hydrogen vacancies in the hydride phase and the fact that the dip is encountered only in desorption isotherms lends support to this explanation.

The reaction taking place in the lower plateau region (H/M = 0.10 to H/M = 0.52) may be written as

$$2.13FeTiH_{0.10} + H_2 \rightleftarrows 2.13FeTiH_{1.04} \quad (1)$$

which is followed by

$$2.20FeTiH_{1.04} + H_2 \rightleftarrows 2.20FeTiH_{1.95} \quad (2)$$

The variation of the log of the equilibrium dissociation pressure with the reciprocal temperature for several solid compositions is shown in Figure 3. The relationship is linear and obeys the van't Hoff equation in the form of $\ln P = (A/T) + B$ where A and B are constants and T is the absolute temperature. Thermodynamic values for the iron titanium–hydrogen system were derived from these data and are shown in Table I. They are given as relative partial molal quantities $(\bar{X}_H - {}^1/_2X°_{H_2})$ where $\bar{X}_H$ is the partial molal enthalpy (entropy or free energy) of hydrogen (as atoms) in the solid, and $X°_{H_2}$ refers to hydrogen in its standard state as a pure, diatomic ideal gas at a pressure of 1 atm.

The products of reactions 1 and 2 are gray metallike solids, essentially not different in appearance from the granular starting alloy. They are very brittle but are not pyrophoric in air; on the contrary, exposure of these materials to air tends to deactivate them and, even though both hydrides have dissociation pressures appreciably above 1 atm at 25°,

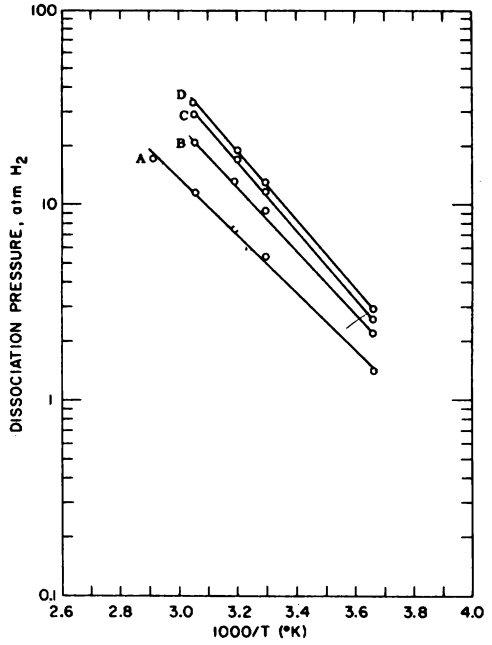

Figure 3. Equilibrium dissociation pressure *vs.* reciprocal temperature for $FeTiH_x$: (A) $FeTiH_{0.1}$–$FeTiH_1$; (B) $FeTiH_{1.2}$; (C) $FeTiH_{1.4}$; (D) $FeTiH_{1.6}$.

they will decompose (*i.e.*, evolve hydrogen) only very slowly in air. Once exposed to air they may be reactivated by repeating the procedure described in the Experimental Section, but a precautionary note should be added here; the remaining hydrided material, though apparently inert, will decompose rapidly into H_2 and FeTi as elevated temperatures are reached (200–300°). Thus the material should not be heated to such temperatures in closed systems unless the free volume is sufficient to accommodate the evolved hydrogen without the buildup of excessive pressure.

As was noted above, iron titanium hydride becomes deactivated upon exposure to air. This property was exploited so that X-ray diffraction patterns of a number of hydride samples could be obtained at 1 atm pressure and room temperature using ordinary powder diffraction techniques and equipment. In order to obtain a suitable sample, iron titanium hydride was prepared in the usual manner. The reactor was then cooled to −196° and evacuated to remove gaseous hydrogen. Air was admitted into the reactor after which it was immediately warmed to room temperature. The reactor was disassembled and a sample for X-ray analysis was taken. The remainder, which was the bulk of the material, was ana-

(7) F. H. Spedding, *et al.*, *Nucleonics*, 4, 4 (1949).
(8) E. Wicke and K. Otto, *Z. Phys. Chem.* (*Frankfurt am Main*), 31, 222 (1962).
(9) G. G. Libowitz and T. R. P. Gibb, *J. Phys. Chem.*, 61, 793 (1957).

Table II. d Spacings for $FeTiH_1$[a]

Line no.	Rel intens[b]	d(obsd), Å	d(calcd), Å	hkl
1	40	2.249	2.249	110
2	20	2.183	2.183	004
3	100	2.145	2.147	103
4	10	1.995	1.999	112
5	50	1.567	1.564	201
6	20	1.284	1.284	204
7	20	1.255	1.247	007

[a] Tetragonal; $a = 3.18$ Å, $c = 8.73$ Å. [b] By visual inspection.

lyzed for hydrogen content by heating it and collecting the evolved hydrogen. If a less then fully hydrided sample was desired, the dihydride was prepared as outlined, but at room temperature (25°) a measured amount of hydrogen was removed from the system to give a sample of the approximate composition desired. The hydride was permitted to reequilibrate at 25° and then was treated as above. Following this procedure we have been able to obtain X-ray diffraction patterns of a number of hydrided samples whose measured compositions ranged from $FeTiH_{0.106}$ to $FeTiH_{1.93}$.

The existence of $FeTiH_1$ was strongly supported by evidence gathered from an examination of the diffraction pattern of a sample whose composition corresponded to $FeTiH_{1.06}$. The pattern was indexed as having tetragonal symmetry with $a = 3.18$ Å and $c = 8.73$ Å, thus giving a c/a ratio of 2.74. There were no reflections present that could be attributed to the FeTi (α) phase. The observed and calculated d spacings are given in Table II. It will be noted in the table that reflections 4 and 5 also appear weakly in the dihydride pattern (discussed below). However, since there are no reflections present which are strong in the latter pattern, the absence of the dihydride may be assumed and both reflections 4 and 5 have been attributed to the monohydride phase. In addition, reflection 5 is fairly strong in the monohydride pattern but weak in the dihydride pattern; further evidence that its placement is correct and proper.

The density of a hydrided sample having composition corresponding to $FeTiH_{0.80}$ was measured under benzene and found to be 6.003 g/cm^3. Since this is a mixture of two phases, hydrogen-saturated FeTi and $FeTiH_1$, and if we take the density of the former as 6.50 g/cm^3 (the known density of FeTi), the density of the latter is calculated to be 5.88 g/cm^3. Knowing the density and using the lattice parameters given above, the number of molecules in a unit cell is calculated to be 2.99 or 3. That the calculated value is so very close to an integral number is substantial evidence that the indexing treatment is correct.

The dihydride phase was also indexed and was found to have a cubic structure. The indexed pattern was obtained using a sample whose composition corresponded to $FeTiH_{1.93}$. For this composition the lattice constant a was found to be 6.61 Å (since this compound is quite nonstoichiometric, the lattice constant is likely to change slightly with hydrogen content). Several of the reflections were very weak and long exposures (~24 hr) were required to define them. It was necessary to use Co Kα radiation, since Cu Kα gives an

Table III. d Spacings for $FeTiH_{1.93}$[a]

Line no.	Rel intens[b]	d(obsd), Å	d(calcd), Å	hkl
1	80	2.320	2.337	220
2	100	2.194	2.203	300, 221
3	50	2.091	2.090	310
4	10	1.994	1.993	311
5	15	1.755	1.766	321
6	10	1.562	1.558	411, 330
7	15	1.416	1.409	332
8	20	1.344	1.349	422
9	10	1.268	1.272	511, 333
10	15	1.210	1.207	521
11	10	1.168	1.168	440
12	10	1.104	1.102	600, 442

[a] Cubic; $a = 6.61$ Å. [b] By visual inspection.

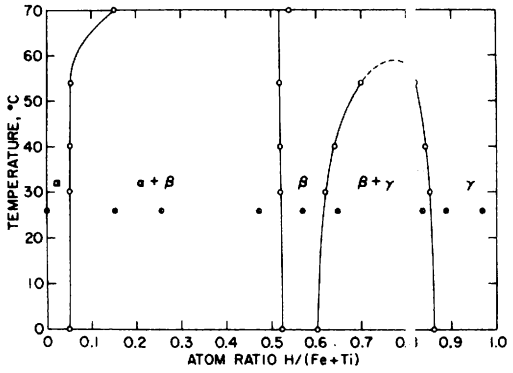

Figure 4. Phase diagram of the FeTi–H system a derived from pressure–composition data. X-Ray diffraction patte ns taken at compositions indicated: •, one solid phase, ⊙, two s lid phases.

appreciable amount of fluorescent radiatio with iron-containing materials which results in a backgro nd on the film against which weak reflections are difficult to detect and measure. The observed and calculated d sp acings for the dihydride phase are shown in Table III. A discussed above reflections 4 and 6 also appear in the mono ydride pattern, but since there is no other evidence of the p resence of the monohydride phase, they have been consid red to be a genuine part of the dihydride pattern. Th density of $FeTiH_{1.93}$, as measured under benzene, was d termined to be 5.47 g/cm^3; using this value and lattice con tant quoted the number of molecules per unit cell was c alculated to be 9.00.

From data abstracted from the pressure–c omposition isotherms discussed above and by using the X-ray diffraction study as ancillary but confirming evidence, a phase diagram of the FeTi–H system has been constructed and is illustrated in Figure 4. The boundaries of the α–β mi ed-phase region are fairly well delineated by the pressure–c mposition isotherms and confirmed broadly by the X-ra data. Unfortunately, the boundaries of β–γ region are n ot so well defined by the pressure–composition data because f the more gradual discontinuities in the isotherms in this com position region.

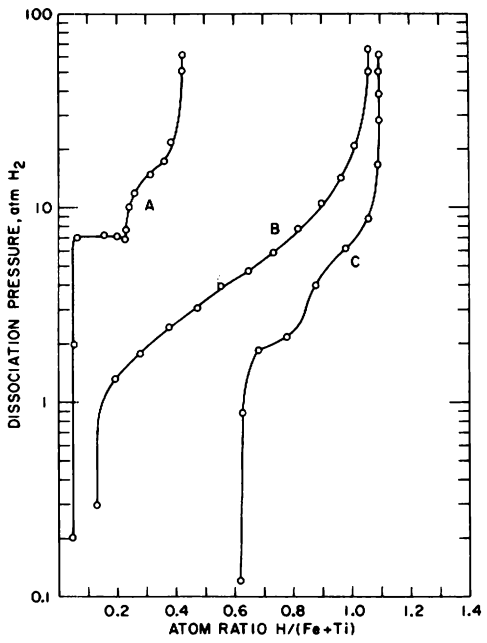

Figure 5. Pressure–composition isotherms for alloys of various Fe/Ti ratios at 40°: 60.5 wt % Fe, 39.5 wt % Ti; (B) 50.5 wt % Fe,-49.2 wt % Ti; (C) 36.7 wt % Fe, 63.2 wt % Ti.

Though carried out only at room temperature, the X-ray data do reflect the phase relationships indicated by the isotherms and add a welcome measure of confidence regarding the location of the phase boundaries for the β–γ region.

The FeTi phase is homogeneous in the composition region extending from 45.9% Ti to 48.2% Ti.[10] The equiatomic composition is 46.17% Ti; thus an appreciable amount of Ti can be dissolved in the intermetallic phase. This fact may be responsible for the behavior illustrated in Figure 5, in which the starting alloy was enriched in Ti to the extent that its initial composition, 49.3% Ti and 50.7% Fe, was slightly above that corresponding to the single-phase region. The isotherm B has been significantly distorted, the equilibrium dissociation pressure markedly decreased, and the boundary between the lower and higher hydride is almost indistinguishable. Such a situation is not without precedent and a somewhat similar effect occurs in the $LaNi_5$–hydrogen system when excess nickel is added to the starting alloy;[11] *i.e.*, the dissociation pressure of the hydride is increased by a factor of over 3 upon increasing the nickel content of the alloy from $LaNi_{4.90}$ to $LaNi_{5.5}$. Thus, in order to obtain reproducible behavior it is advisable to control the intermetallic composition as closely as possible. Upon increasing the Ti content to 63.2%, the pressure–composition isotherm C is greatly distorted as also shown in Figure 5. This alloy was annealed at 1000° for 12 hr and then quenched in an unsuccessful attempt to prepare metastable $FeTi_2$; but only FeTi and Ti were produced. After hydriding, an X-ray diffraction pattern of the product indicated the presence of $FeTiH_{\sim 2}$, $TiH_{\sim 2}$, FeTi, and Ti. The increased amount of residual hydrogen in the solid is undoubtedly due to the presence of the stable titanium hydride.

Upon departing from the single-phase region in the opposite direction, *i.e.*, that of higher iron content, there appears to be no significant effect other than a reduction in the amount of hydrogen sorbed as shown in Figure 5. The starting alloy was a two-phase mixture, Fe_2Ti and FeTi, having an overall composition of 60.5 wt % Fe and 39.5 wt % Ti. The isotherm A is essentially congruent with that obtained with FeTi, indicating little interaction between the two phases or solid solubility of Fe in FeTi; an observation which is in accord with the known homogeneity range of FeTi. The amount of hydrogen actually sorbed is somewhat less than that expected from the proportionate amount of FeTi present in the alloy, which may be due to the mere physical presence of Fe_2Ti.

Acknowledgment. The authors wish to express their thanks to Messrs. J. Hughes and A. Holtz for their expert assistance in the laboratory.

Registry No. FeTiH, 39433-91-5; $FeTiH_2$, 39433-92-6; 37–70% Fe, 30–63% Ti, 39433-89-1; H_2, 1333-74-0; FeTi, 12023-04-0; Fe, 7439-89-6; Ti, 7440-32-6.

(10) W. R. Pearson, "Handbook of Lattice Spacings and Structures of Metals," Vol. 2, Pergamon Press, London, 1967, p 242.

(11) K. H. J. Buschow and H. H. Van Mal, *J. Less-Common Metals*, 29, 203 (1972).

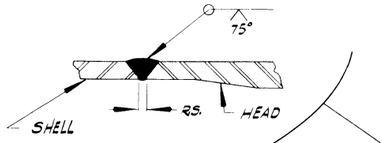

12" WELDING CAP SCH 40 316 SS TYP. BOTH ENDS

6'-6" ±

R.S.

5'-6" SHELL LENGTH

R.S.

12" SCH. 20 PIPE (WELDED) 316 SS

SKIRT $\frac{1}{4} \times 1\frac{1}{2}$ 304 SS

F.R.

TEN(10) SWAGELOK BUTT WELD MALE CONNECTOR PART# 600-1-8W-316

PLUG WELD 6 PLACES 120° APART

7" DIA.

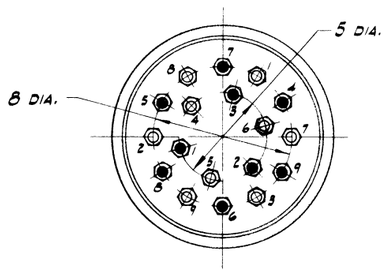

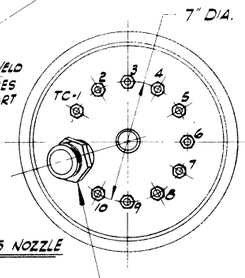

3

ACCESS NOZZLE

TYP. F.R.

$\frac{1}{4}$ I-3 TYP.

ONE (1) CPV UNION PART # H849-24-SS + BLANK TAILPIECE & NUT

NOTE:
DARKENED AREAS ARE WATER INLET TUBES

EIGHTEEN (18) SWAGELOK BUTT WELD MALE CONNECTOR PART# 1010-1-8W-316

$2\frac{1}{2} \times 1$ REDUCER SCH 40 316 SS

PMT $\frac{5}{8}$ O.D. X $\frac{1}{16}$ W. $\frac{1}{2}$ MICRON, 316 SS (6 REQ'D.)

1" SCH 40 PIPE 316 SS

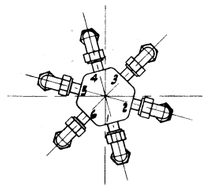

GAS INLET

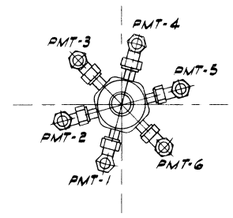

SIX(6) SWAGELOK UNION ELBOW PART# 1010-9-316

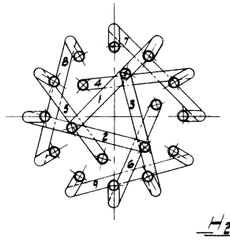

G.P. #1 — 8 — G.P. #2 — 18 — G.P. #3 — 20 — G.P. #4 — 18

W.L.

U-TUBE $\frac{5}{8}$ O.D. x .049 W. 304 SS (9 REQ'D.)

3" R. TYP.

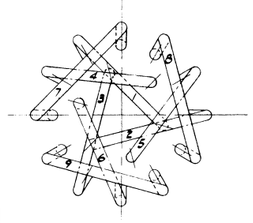

$2\frac{1}{2}$ 21R.

H_2O HEAT TRANSFER TUBE

21R

U-TUBE	"X"
1, 2, 3	1
4, 5, 6	9/64
7, 8, 9	15/64

U-TUBE	ANGLE ∝
1, 2, 3	14.6°
4, 5, 6	23.2°
7, 8, 9	45°

VESSEL DATA

DESIGN PRESSURE - 633 PSIG
DESIGN TEMP - -20 TO 200°F
HYDROS. TEST - 950 PSIG
RADIOGRAPH - 100% - LONG. JOINT ON SHELL & HEAD TO SHELL JOINTS
WELDING PROCESS - TIG

NO. REQ.	ACCT. NO.	I.L.R. NO.	ORDER NO.	DEPT.	JOB NUMBER	USED ON DWG. NO.	NO. PER. ASS'Y.
DEC. ± ANG. ± TOLERANCE			MAX. MIN. BREAK SHARP EDGES		BROOKHAVEN NATIONAL LABORATORY ASSOCIATED UNIVERSITIES, INC. UPTON, N. Y. 11973		
0-20" 20"-60" OVER 60" FRACTIONAL TOLERANCE				FINISH √	10" HYDROGEN RESERVOIR VESSEL		
MAR. 28, 74 DATE	ST. STL. AS NOTED MATERIAL		1/4" = 1" SCALE	WEIGHT	ASSEMBLY & DETAILS		
H. PETERS DRAWN BY	CHECKED BY		ENG. APP.	SUPVR. APP.	ME-13.2-1 -4 DRAWING NUMBER		A REV

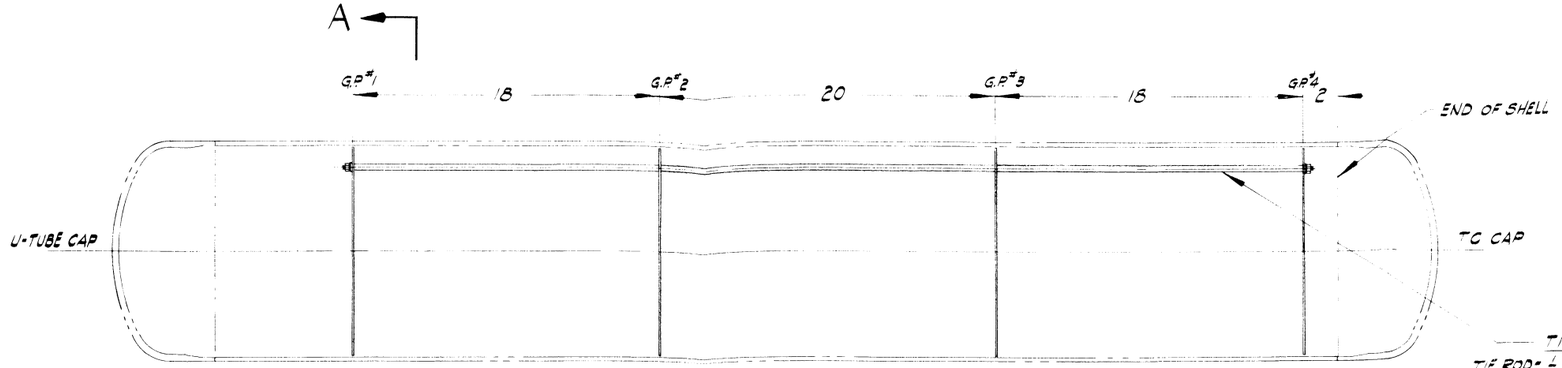

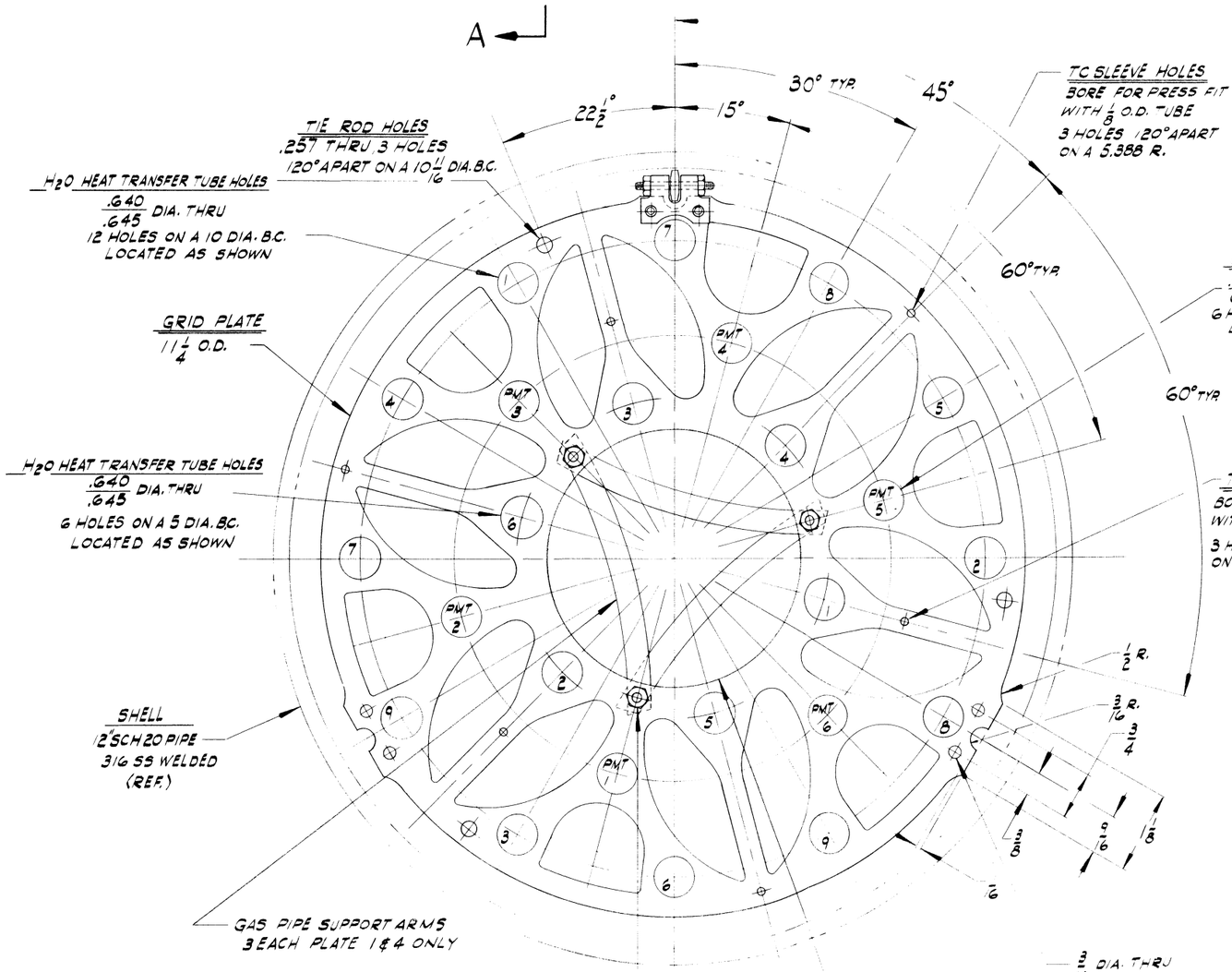

VIEW A-A

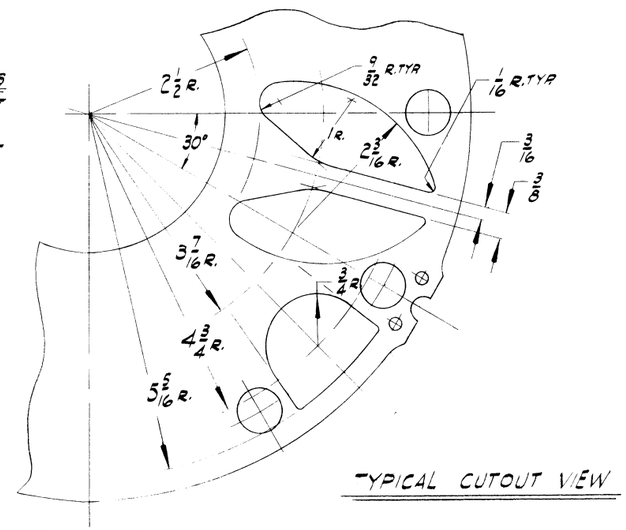

TYPICAL CUTOUT VIEW

NO. REQ.	ACCT. NO.	I.L.R. NO.	ORDER NO.	DEPT.	JOB NUMBER	USED ON DWG. NO.	NO. PER ASS'Y.

DEC. ± / ANG. ± TOLERANCE		MAX. / MIN. BREAK SHARP EDGES	
0-20" / 20"-60" / OVER 60" FRACTIONAL TOLERANCE			FINISH ✓
4-17-74	304 S.S. 1/8 THK	1/4 & FULL	
DATE	MATERIAL	SCALE	WEIGHT
H. PETERS	SJM/		SJM
DRAWN BY	CHECKED BY	ENG. APP.	SUPVR. APP.

BROOKHAVEN NATIONAL LABORATORY
ASSOCIATED UNIVERSITIES, INC.
UPTON, N. Y. 11973

0" HYDROGEN RESERVOIR VESSEL
GRID PLATE #1
DETAIL & LOCATIONS

ME-13.2-2 -4 | A
DRAWING NUMBER | REV